Chiral symmetry and the nucleon spin structure functions

M. Wakamatsu* and T. Kubota†
Department of Physics, Faculty of Science, Osaka University, Toyonaka, Osaka 560, Japan
(Received 17 September 1998; published 8 July 1999)

We carry out a systematic investigation of twist-two spin dependent structure functions of the nucleon within the framework of the chiral quark soliton model (CQSM) by paying special attention to the role of chiral symmetry of QCD. The importance of chiral symmetry is illustrated through the good reproduction of the recent SLAC data for the neutron spin structure function $g_1^n(x,Q^2)$. We also observe a substantial difference between the predictions of the longitudinally polarized distribution functions and those of the transversity distribution functions. That the chiral symmetry may be responsible for this difference is seen in the isospin dependence of the corresponding first moments, i.e., the axial and tensor charges. The CQSM predicts $g_A^{(0)}/g_A^{(3)} \simeq 0.25$ for the ratio of the isoscalar to isovector axial charges, while $g_T^{(0)}/g_T^{(3)} \simeq 0.46$ for the ratio of the isoscalar to isovector tensor charges, which should be compared with the prediction $g_A^{(0)}/g_A^{(3)} = g_T^{(0)}/g_T^{(3)} = 3/5$ of the constituent quark model or of the naive MIT bag model without proper account of chiral symmetry. Another prominent prediction of the CQSM is the opposite polarization of the $\bar{u}$ and $\bar{d}$ antiquarks, thereby indicating the SU(2) asymmetric sea quark (spin) polarization in the nucleon.
[S0556-2821(99)06813-7]

PACS number(s): 13.60.Hb, 12.39.Fe, 12.39.Ki

I. INTRODUCTION

Undoubtedly, the so-called ''nucleon spin crisis'' caused by the European Muon Collaboration (EMC) measurement in 1988 is one of the most exciting topics in the field of hadron physics [1]. The recent renaissance of nucleon structure function physics is greatly indebted to this epoch-making finding. Naturally, the physics of nucleon structure functions has two different aspects. One is a perturbative aspect, while the other is a nonperturbative aspect. Because of the asymptotic freedom of QCD, the Q^2 evolution of quark distribution functions can be controlled by the perturbative QCD at least for large enough Q^2 [2]. However, perturbative QCD is entirely powerless for predicting distribution functions themselves. Here we need to solve nonperturbative QCD in some way. Unfortunately, we have no reliable analytical method for handling this aspect of QCD. For the present moment, we are then left with two tentative choices. One is to rely upon lattice QCD, while the other is to use effective models of QCD. If one takes the first choice, one must first evaluate infinite towers of moments of distribution functions, since the direct calculation of distribution functions does not match this numerical simulation method [3]. Here we take the second choice, which allows us a direct calculation of quark distribution functions. Still, there are quite a lot of effective models of baryons. We advocate that the chiral quark soliton model (CQSM) is a unique model of baryons which has several appealing features not possessed by other models of baryons, especially when applied to the physics of quark distribution functions. First of all, it is an effective model of baryons maximally incorporating spontaneous chiral symmetry breaking of QCD vacuum [4–6]. The nucleon in this model is a composite of three valence quarks and infinitely many Dirac sea quarks moving in a slowly rotating M.F. of hedgehog shape. As a natural consequence, it automatically simulates cloud of pions surrounding the core of three valence quarks. Nevertheless, since everything is described in terms of effective quark fields only, we need not worry about a double counting of quark and pion degrees of freedom. (We recall that this kind of double counting occurs, for instance, in models of hadrons based on the linear-sigma-quark-model type Lagrangian [7,8].) This also means that we do not need to use such an ambiguous procedure as convoluting the pion structure functions with *pion probability function* (or more precisely a light-cone momentum distribution of the pion) inside the nucleon [9–11].

Several group have already attempted to calculate nucleon structure functions within the CQSM or the Nambu–Jona-Lasinio (NJL) soliton model. For instance, Weigel *et al.* investigated the polarized as well as unpolarized structure functions of the nucleon under the so-called ''valence quark approximation'' [12]. This is not an extremely bad approximation, but it is known to have several unpleasant features. Probably, most serious would be the violation of positivity condition for the unpolarized antiquark (or sea quark) distribution functions. Although such an apparent disaster does not happen for the spin dependent quark distribution functions, a lesson learned from the above observation is that a reliable prediction of *antiquark* distributions would not be obtainable unless incorporating effects of Dirac sea quarks or equivalently vacuum polarization effects.

More consistent calculation including vacuum polarization effects have been performed by Diakonov *et al.* [13,14] and also by Tanikawa and Saito [15] with different regularization schemes, but by confining to the isosinglet unpolarized as well as isovector longitudinally polarized distribution functions, which have values at the leading order of $1/N_c$ expansion (or at the 0th order of the expansion in the collective angular velocity Ω of the hedgehog soliton). Unfortu-

*Email address: wakamatu@miho.rcnp.osaka-u.ac.jp
†Email address: kubota@kern.phys.sci.osaka-u.ac.jp

nately, an abundance of interesting physics like the physics of ''nucleon spin contents'' is contained in the next order of $1/N_c$ expansion [5]. This is easily understood because the inclusion of $O(\Omega^1)$ terms is the minimum condition for the collective quantization treatment of hedgehog solitons to hold. Otherwise, the nucleon cannot have correct quantum numbers [4–6].

We have recently reported the first calculation of the $O(\Omega^1)$ contributions to the isovector unpolarized quark distribution function related to the physics of Gottfried sum [16] with full inclusion of the vacuum polarization effects [17]. It was shown that the model can explain the excess of the $\bar{d}$ sea over the $\bar{u}$ sea in the proton very naturally [17–19]. However, some of the treatments there were criticized in a recent paper by Pobylitsa *et al.* [20]. In the process of obtaining theoretical quark distribution functions, we need to evaluate nucleon matrix elements of quark bilinear operators which are nonlocal in time. Their criticism is that the calculation in [17] does not treat this nonlocality in time to the full extent.

Now the purpose of the present paper is to carry out a systematic calculation of all the twist-2 spin dependent quark distribution functions of the nucleon as consistently as possible. We evaluate both of the $O(\Omega^0)$ and $O(\Omega^1)$ contributions with full inclusion of the vacuum polarization effects. The above-mentioned nonlocality effects are also carefully taken into account. We believe that these unique features of our theoretical analysis would give new and important information on the nonperturbative aspect of the spin dependent quark distribution functions including the *antiquark* distributions as well.

The plan of the paper is as follows. For completeness, we give in Sec. II a precise definition of twist-2 quark distribution functions which we shall investigate in the present paper. How to evaluate these quark distribution functions within the framework of the CQSM is explained in Sec. III. Section IV is devoted to the discussion of the numerical results. We then summarize what we have found in Sec. V.

II. DEFINITION OF QUARK DISTRIBUTION FUNCTIONS

Most theoretical analyses of quark distribution functions of the nucleon are based on a field-theoretical formulation given by Collins and Soper [21]. As a natural extension, Jaffe and Ji recently carried out a systematic classification of quark distribution functions by including chiral-odd distribution functions which do not appear in the formulas of deep inelastic scattering cross sections [22]. According to them, there are nine independent distribution functions, from twist 2 to twist 4. Here we are interested in the twist-2 distribution functions, which are known to have simple parton model interpretation. There are three twist-2 distribution functions, the spin independent (or averaged) distribution $f_1(x)$, the longitudinally polarized distribution $g_1(x)$, and what is called the transversity distribution $h_1(x)$. Following the notation of [22], they are represented as

$$f_1(x)=\frac{1}{\sqrt{2}p^+}\int\frac{d\lambda}{2\pi}e^{i\lambda x}\langle PS|\psi_+^\dagger(0)\psi_+(\lambda n)|PS\rangle, \quad (1)$$

$$g_1(x)=\frac{1}{\sqrt{2}p^+}\int\frac{d\lambda}{2\pi}e^{i\lambda x}\langle PS_z|\psi_+^\dagger(0)\gamma_5\psi_+(\lambda n)|PS_z\rangle, \quad (2)$$

$$h_1(x)=\frac{1}{\sqrt{2}p^+}\int\frac{d\lambda}{2\pi}\times e^{i\lambda x}\langle PS_\perp|\psi_+^\dagger(0)\gamma_\perp\gamma_5\psi_+(\lambda n)|PS_\perp\rangle, \quad (3)$$

where p^μ and n^μ are two lightlike (null) vectors, having the properties,

$$p^-=0,\ \ n^+=0,\ \ p^2=n^2=0,\ \ p\cdot n=1. \quad (4)$$

Without loss of generality, one can choose a frame in which the four-momentum P^μ of the initial nucleon and the four-momentum transfer q^μ from a lepton to a nucleon have the third and the time components only. In this frame, p^μ and n^μ take the form

$$p^\mu=\frac{\mathcal{P}}{\sqrt{2}}(1,0,0,1),\ \ n^\mu=\frac{1}{\sqrt{2}\mathcal{P}}(1,0,0,-1), \quad (5)$$

while P^μ and q^μ are represented as

$$P^\mu=p^\mu+\frac{M^2}{2}n^\mu, \quad (6)$$

$$q^\mu=\frac{1}{M_N^2}(\nu-\sqrt{\nu^2+M_N^2Q^2})p^\mu+\frac{1}{2}(\nu+\sqrt{\nu^2+M_N^2Q^2})n^\mu, \quad (7)$$

with $\nu=P\cdot q$ and $Q^2=-q^2$. In the above definition of the twist-2 quark distribution functions, ψ_+ is a component of the quark field ψ defined through the decomposition

$$\psi=(P_++P_-)\psi=\psi_++\psi_-, \quad (8)$$

by the projection operators $P_\pm=\frac{1}{2}\gamma^\mp\gamma^\pm$ with $\gamma^\pm=(1/\sqrt{2})(\gamma^0\pm\gamma^3)$. According to the authors of [22], ψ_+ is called the ''good'' component of ψ, since it describes an independent propagating degrees of freedom in the light-cone quantization scheme [23]. On the other hand, ψ_- is called the ''bad'' component, since it can be interpreted as quark-gluon composites. It is important to recognize that only the good component of ψ appears in the definition of twist-2 quark distribution functions in conformity with the fact that they have simple parton model interpretation. In the actual model calculation of these distribution functions, it is more convenient to rewrite the above expressions with use of the identities

$$P_+^2=P_+=\frac{1}{2}(1+\gamma^0\gamma^3), \quad (9)$$

$$P_+\gamma_5 P_+ = \frac{1}{2}(1+\gamma^0\gamma^3)\gamma_5, \tag{10}$$

$$P_+\gamma_\perp\gamma_5 P_+ = \frac{1}{2}(1+\gamma^0\gamma^3)\gamma_\perp\gamma_5. \tag{11}$$

Since the distribution functions are in principle frame-independent, it is also convenient to go to the nucleon rest frame, in which one can set $\mathcal{P}=M_N/\sqrt{2}$. Now using the change of variable as

$$\lambda n^\mu = \lambda\frac{1}{M_N}(1,0,0,-1)\equiv z^\mu, \tag{12}$$

we obtain

$$z_0=\frac{\lambda}{M_N},\quad z_3=-\frac{\lambda}{M_N}=-z_0,\quad z_\perp=0. \tag{13}$$

Noting that

$$\int_{-\infty}^{\infty} d\lambda\, e^{i\lambda x}\cdots = M_N\int_{-\infty}^{\infty} dz_0 e^{ixM_N z_0}\cdots, \tag{14}$$

we are then led to the following expressions:

$$f_1(x)=\frac{1}{4\pi}\int dz^0 e^{ixM_N z_0}\langle \boldsymbol{P}=0,S|\psi^\dagger(0)(1+\gamma^0\gamma^3)\psi(z)|\boldsymbol{P}=0,S\rangle|_{z_3=-z_0,z_\perp=0}, \tag{15}$$

$$g_1(x)=\frac{1}{4\pi}\int dz^0 e^{ixM_N z_0}\langle \boldsymbol{P}=0,S_z|\psi^\dagger(0)(1+\gamma^0\gamma^3)\gamma_5\psi(z)|\boldsymbol{P}=0,S_z\rangle|_{z_3=-z_0,z_\perp=0}, \tag{16}$$

$$h_1(x)=\frac{1}{4\pi}\int dz^0 e^{ixM_N z_0}\langle \boldsymbol{P}=0,S_\perp|\psi^\dagger(0)(1+\gamma^0\gamma^3)\gamma_\perp\gamma_5\psi(z)|\boldsymbol{P}=0,S_\perp\rangle|_{z_3=-z_0,z_\perp=0}. \tag{17}$$

What is left for us now is to evaluate nucleon matrix elements of quark bilinear operators containing two space-time coordinates with light-cone distance. How to evaluate these matrix elements of *bilocal* quark operators will be explained in the next section.

III. THEORY OF QUARK DISTRIBUTION FUNCTIONS

As shown in the previous section, the quark distribution functions of our present interest can generally be represented in the form

$$q(x)=\frac{1}{4\pi}\int_{-\infty}^{\infty} dz_0 e^{ixM_N z_0}\langle N(\boldsymbol{P}=0)\times|\psi^\dagger(0)O_a\psi(z)|N(\boldsymbol{P}=0)\rangle|_{z_3=-z_0,z_\perp=0}. \tag{18}$$

In the present study, we confine to spin-dependent distribution functions, so that we are to take

$$O_a=(1+\gamma^0\gamma^3)\gamma_5,\quad \tau_3(1+\gamma^0\gamma^3)\gamma_5, \tag{19}$$

respectively for the isoscalar and isovector parts of the longitudinally polarized distribution functions, whereas

$$O_a=(1+\gamma^0\gamma^3)\gamma_\perp\gamma_5,\quad \tau_3(1+\gamma^0\gamma^3)\gamma_\perp\gamma_5, \tag{20}$$

for the isoscalar and isovector parts of the transversity distributions. We recall here the fact that, extending the definition of distribution function $q(x)$ to interval $-1\leqslant x\leqslant 1$, the relevant antiquark distributions are given as [14]

$$\Delta\bar{u}(x)+\Delta\bar{d}(x)=\Delta u(-x)+\Delta d(-x)\quad (0<x<1), \tag{21}$$

$$\Delta\bar{u}(x)-\Delta\bar{d}(x)=\Delta u(-x)-\Delta d(-x)\quad (0<x<1), \tag{22}$$

for the longitudinally polarized distributions, while

$$\delta\bar{u}(x)+\delta\bar{d}(x)=-[\delta u(-x)+\delta d(-x)]\quad (0<x<1), \tag{23}$$

$$\delta\bar{u}(x)-\delta\bar{d}(x)=-[\delta u(-x)-\delta d(-x)]\quad (0<x<1), \tag{24}$$

for the transversity distributions [22]. As explained in the previous paper [17], the basis of our analysis is the following path integral representation of a matrix element of an arbitrary (bilocal) quark bilinear operator between the nucleon states with definite momenta:

$$\begin{aligned}\langle N(\boldsymbol{P})|\psi^\dagger(0)O_a\psi(z)|N(\boldsymbol{P})\rangle &= \frac{1}{Z}\int d^3x d^3y e^{-i\boldsymbol{P}\cdot\boldsymbol{x}}e^{i\boldsymbol{P}\cdot\boldsymbol{y}}\int\mathcal{D}U\int\mathcal{D}\psi\mathcal{D}\psi^\dagger \\ &\times J_N\left(\frac{T}{2},\boldsymbol{x}\right)\psi^\dagger(0)O_a\psi(z)J_N^\dagger\left(-\frac{T}{2},\boldsymbol{y}\right) \\ &\times\exp\left[i\int d^4x\,\bar{\psi}(i\partial\!\!\!/-MU^{\gamma_5})\psi\right],\end{aligned} \tag{25}$$

where

$$\mathcal{L}=\bar{\psi}(i\partial\!\!\!/-MU^{\gamma_5}(x))\psi, \tag{26}$$

with $U^{\gamma_5}(x)=\exp[i\gamma_5\boldsymbol{\tau}\cdot\boldsymbol{\pi}(x)/f_\pi]$ being the basic Lagrangian of the CQSM, and

$$J_N(x)=\frac{1}{N_c!}\epsilon^{\alpha_1\cdots\alpha_{N_c}}\Gamma^{\{f_1\cdots f_{N_c}\}}_{JJ_3,TT_3}\psi_{\alpha_1 f_1}(x)\cdots\psi_{\alpha_{N_c}f_{N_c}}(x) \tag{27}$$

is a composite operator carrying the quantum numbers JJ_3,TT_3 (spin, isospin) of the nucleon, where α_i is the color index, while $\Gamma^{\{f_1\cdots f_{N_c}\}}_{JJ_3,TT_3}$ is a symmetric matrix in spin-flavor indices f_i. By starting with a stationary pion field configu-

ration of hedgehog shape $U_0^{\gamma_5}(\boldsymbol{x})=\exp[i\gamma_5\boldsymbol{\tau}\cdot\hat{\boldsymbol{r}}F(r)]$, the path integral over the pion fields U can be done in a saddle point approximation. Next, we consider two important fluctuations around the static configuration, i.e., the translational and rotational zero modes. To treat the translational zero-modes, we use an approximate momentum projection procedure of the nucleon state, which amounts to integrating over all shift $\boldsymbol{R}$ of the soliton center-of-mass coordinates [14]:

$$\langle N(\boldsymbol{P})|\psi^\dagger(0)O_a\psi(z)|N(\boldsymbol{P})\rangle \to\int d^3R\langle N(\boldsymbol{P})|\psi^\dagger(0,-\boldsymbol{R})O_a\psi(z_0,\boldsymbol{z}-\boldsymbol{R})|N(\boldsymbol{P})\rangle. \tag{28}$$

The rotational zero modes can be treated by introducing a rotating meson field of the form

$$U^{\gamma_5}(\boldsymbol{x},t)=A(t)U_0^{\gamma_5}(\boldsymbol{x})A^\dagger(t), \tag{29}$$

where $A(t)$ is a time-dependent $SU(2)$ matrix in the isospin space. Note first the identity

$$\bar{\psi}(i\partial\!\!\!/-MA(t)U_0^{\gamma_5}(\boldsymbol{x})A^\dagger(t))\psi=\psi_A^\dagger(i\partial_t-H-\Omega)\psi_A, \tag{30}$$

with

$$\psi_A=A^\dagger(t)\psi,\ \ H=\frac{\boldsymbol{\alpha}\cdot\nabla}{i}+M\beta U_0^{\gamma_5}(\boldsymbol{x}),\ \ \Omega=-iA^\dagger(t)\dot{A}(t). \tag{31}$$

Here H is a static Dirac Hamiltonian with the background pion fields $U_0^{\gamma_5}(\boldsymbol{x})$, playing the role of a mean field for quarks, while $\Omega=\frac{1}{2}\Omega_a\tau_a$ is the SU(2)-valued angular velocity matrix later to be quantized as $\Omega_a\to\hat{J}_a/I$ with I the moment of inertia of the soliton and $\hat{J}_a$ the angular momentum operator [4–6]. We then introduce a change of quark field variables $\psi\to\psi_A$, which amounts to getting on a body-fixed rotating frame. Denoting ψ_A anew as ψ for notational simplicity, the nucleon matrix element (25) can then be written as

$$\langle N(\boldsymbol{P})|\psi^\dagger(0)O_a\psi(z)|N(\boldsymbol{P})\rangle=\frac{1}{Z}\Gamma^{\{f\}}\Gamma^{\{g\}*}\int d^3xd^3ye^{-i\boldsymbol{P}\cdot\boldsymbol{x}}e^{i\boldsymbol{P}\cdot\boldsymbol{y}}\int d^3R\int\mathcal{D}A\mathcal{D}\psi\mathcal{D}\psi^\dagger\exp\left[i\int d^4x\psi^\dagger(i\partial_t-H-\Omega)\psi\right]$$
$$\times\prod_{i=1}^{N_c}\left[A\left(\frac{T}{2}\right)\psi_{f_i}\left(\frac{T}{2},\boldsymbol{x}\right)\right]\psi^\dagger(0,-\boldsymbol{R})A^\dagger(0)O_aA(z_0)\psi(z_0,\boldsymbol{z}-\boldsymbol{R})\prod_{j=1}^{N_c}\left[\psi_{g_j}^\dagger\left(-\frac{T}{2},\boldsymbol{y}\right)A^\dagger\left(-\frac{T}{2}\right)\right]. \tag{32}$$

Now performing the path integral over the quark fields, we obtain

$$\langle N(\boldsymbol{P})|\psi^\dagger(0)O_a\psi(z)|N(\boldsymbol{P})\rangle=\frac{1}{Z}\tilde{\Gamma}^{\{f\}}\tilde{\Gamma}^{\{g\}^\dagger}N_c\int d^3xd^3ye^{-i\boldsymbol{P}\cdot\boldsymbol{x}}e^{i\boldsymbol{P}\cdot\boldsymbol{y}}\int d^3R\int\mathcal{D}A\Bigg\{{}_{f_1}\left\langle\frac{T}{2},\boldsymbol{x}\left|\frac{i}{i\partial_t-H-\Omega}\right|0,-\boldsymbol{R}\right\rangle_\gamma\cdot(A^\dagger(0)$$
$$\times O_aA(z_0))_{\gamma\delta}\cdot{}_\delta\left\langle z_0,\boldsymbol{z}-\boldsymbol{R}\left|\frac{i}{i\partial_t-H-\Omega}\right|-\frac{T}{2},\boldsymbol{y}\right\rangle_{g_1}$$
$$-\mathrm{Tr}\left(\left\langle z_0,\boldsymbol{z}-\boldsymbol{R}\left|\frac{i}{i\partial_t-H-\Omega}\right|0,-\boldsymbol{R}\right\rangle A^\dagger(0)O_aA(z_0)\right)_{f_1}\left\langle\frac{T}{2},\boldsymbol{x}\left|\frac{i}{i\partial_t-H-\Omega}\right|-\frac{T}{2},\boldsymbol{y}\right\rangle_{g_1}\Bigg\}$$
$$\times\prod_{j=2}^{N_c}\left[{}_{f_j}\left\langle\frac{T}{2},\boldsymbol{x}\left|\frac{i}{i\partial_t-H-\Omega}\right|-\frac{T}{2},\boldsymbol{y}\right\rangle_{g_j}\right]\cdot\exp[N_c\mathrm{Sp}\log(i\partial_t-H-\Omega)], \tag{33}$$

with $\tilde{\Gamma}^{\{f\}}=\Gamma^{\{f\}}[A(T/2)]^{N_c}$ etc. Here Tr is to be taken over spin-flavor indices. Assuming a slow rotation of the hedgehog soliton, we can make use of an expansion in Ω. Since Ω is known to be an $O(1/N_c)$ quantity, this perturbative expansion in Ω can also be taken as a $1/N_c$ expansion. For an effective action, this gives

$$\mathrm{Sp}\log(i\partial_t-H-\Omega)=\mathrm{Sp}\log(i\partial_t-H)+i\frac{1}{2}I\int\Omega_a^2dt. \tag{34}$$

The second term here is essentially the action of a rigid rotor, which plays the role of the evolution operator in the space of collective coordinates. We also use the expansion of the single quark propagator as

$$
{}_{f_1}\left\langle \frac{T}{2},\boldsymbol{x}\left|\frac{i}{i\partial_t-H-\Omega}\right|0,-\boldsymbol{R}\right\rangle_{\gamma}
={}_{f_1}\left\langle \frac{T}{2},\boldsymbol{x}\left|\frac{i}{i\partial_t-H}\right|0,-\boldsymbol{R}\right\rangle_{\gamma}
-\int dz_0' d^3z'\,{}_{f_1}\left\langle \frac{T}{2},\boldsymbol{x}\left|\frac{i}{i\partial_t-H}\right|z_0',\boldsymbol{z}'\right\rangle_{\alpha}\cdot i\Omega_{\alpha\beta}(z_0')\cdot{}_{\beta}\left\langle z_0',\boldsymbol{z}'\left|\frac{i}{i\partial_t-H}\right|0,-\boldsymbol{R}\right\rangle_{\gamma}+\cdots . \tag{35}
$$

An important suggestion made in a recent paper by Pobilytsa *et al.* [20] is that one must also take account of the nonlocality (in time) of the operator $A^{\dagger}(0)O_aA(z_0)$. Expanding this operator around 0 or z_0, one respectively obtains

$$
A^{\dagger}(0)O_aA(z_0)=A^{\dagger}(0)O_aA(0)+z_0A^{\dagger}(0)O_a\dot{A}(0)+\cdots , \tag{36}
$$

$$
\text{or}\quad A^{\dagger}(0)O_aA(z_0)=A^{\dagger}(z_0)O_aA(z_0)-z_0\dot{A}^{\dagger}(z_0)O_aA(z_0)+\cdots . \tag{37}
$$

Since both choices are known to lead to the same answer [20], it is convenient to use a symmetrized form in the following manipulation. This amounts to performing the following replacement:

$$
A^{\dagger}(0)O_aA(z_0)\rightarrow A^{\dagger}O_aA+\frac{1}{2}z_0(A^{\dagger}O_aAA^{\dagger}\dot{A}-\dot{A}^{\dagger}AA^{\dagger}O_aA),
$$

$$
=\tilde{O}_a+iz_0\frac{1}{2}\{\Omega,\tilde{O}_a\}, \tag{38}
$$

in the process of collective quantization of the rotational motion. Here we have introduced the notation

$$
\tilde{O}_a\equiv A^{\dagger}O_aA, \tag{39}
$$

for saving space. Equation (38) means that the nonlocality of the operator $A^{\dagger}(0)O_aA(z_0)$ causes a rotational correction *proportional* to the collective angular velocity Ω. After taking all these into account, we are then led to a perturbative series in Ω, which is also regarded as a $1/N_c$ expansion:

$$
\langle N(\boldsymbol{P})|\psi^{\dagger}(0)O_a\psi(z)|N(\boldsymbol{P})\rangle=\langle N(\boldsymbol{P})|\psi^{\dagger}(0)O_a\psi(z)|N(\boldsymbol{P})\rangle^{\Omega^0}+\langle N(\boldsymbol{P})|\psi^{\dagger}(0)O_a\psi(z)|N(\boldsymbol{P})\rangle^{\Omega^1}+\cdots , \tag{40}
$$

where

$$
\begin{aligned}
\langle N(\boldsymbol{P})|\psi^{\dagger}(0)O_a\psi(z)|N(\boldsymbol{P})\rangle^{\Omega^0}=\frac{1}{Z}\tilde{\Gamma}^{\{f\}}\tilde{\Gamma}^{\{g\}^{\dagger}}N_c\int d^3xd^3ye^{-i\boldsymbol{P}\cdot\boldsymbol{x}}e^{i\boldsymbol{P}\cdot\boldsymbol{y}}\int d^3R\int \mathcal{D}A(\tilde{O}_a)_{\gamma\delta}&\\
\times\Bigg[{}_{f_1}\left\langle \frac{T}{2},\boldsymbol{x}\left|\frac{i}{i\partial_t-H}\right|0,-\boldsymbol{R}\right\rangle_{\gamma}\cdot{}_{\delta}\left\langle z_0,\boldsymbol{z}-\boldsymbol{R}\left|\frac{i}{i\partial_t-H}\right|-\frac{T}{2},\boldsymbol{y}\right\rangle_{g_1}&\\
-{}_{\delta}\left\langle z_0,\boldsymbol{z}-\boldsymbol{R}\left|\frac{i}{i\partial_t-H}\right|0,-\boldsymbol{R}\right\rangle_{\gamma}\cdot{}_{f_1}\left\langle \frac{T}{2},\boldsymbol{x}\left|\frac{i}{i\partial_t-H}\right|-\frac{T}{2},\boldsymbol{y}\right\rangle_{g_1}\Bigg]&\\
\times\prod_{j=2}^{N_c}\left[{}_{f_j}\left\langle \frac{T}{2},\boldsymbol{x}\left|\frac{i}{i\partial_t-H}\right|-\frac{T}{2},\boldsymbol{y}\right\rangle_{g_j}\right]\cdot\exp\left[N_c,\mathrm{Sp}\log(i\partial_t-H)+i\frac{I}{2}\int\Omega_a^2dt\right],&
\end{aligned}
\tag{41}
$$

and

$$
\begin{aligned}
&\langle N(\boldsymbol{P})|\psi^\dagger(0)O_a\psi(z)|N(\boldsymbol{P})\rangle^{\Omega^1}\\
&=\frac{1}{Z}\tilde{\Gamma}^{\{f\}}\tilde{\Gamma}^{\{g\}\dagger}N_c\int d^3x d^3y e^{-i\boldsymbol{P}\cdot\boldsymbol{x}}e^{i\boldsymbol{P}\cdot\boldsymbol{y}}\int d^3R\int\mathcal{D}\mathcal{A}\Bigg\{\int d^3z' dz_0' i\Omega_{\alpha\beta}(z_0')(A^\dagger(0)O_aA(z_0))_{\gamma\delta}\\
&\times\Bigg[{}_{f_1}\left\langle\frac{T}{2},\boldsymbol{x}\left|\frac{i}{i\partial_t-H}\right|z_0',\boldsymbol{z}'\right\rangle_{\alpha\ \beta}\cdot\left\langle z_0',\boldsymbol{z}'\left|\frac{i}{i\partial_t-H}\right|0,-\boldsymbol{R}\right\rangle_{\gamma\ \delta}\cdot\left\langle z_0,\boldsymbol{z}-\boldsymbol{R}\left|\frac{i}{i\partial_t-H}\right|-\frac{T}{2},\boldsymbol{y}\right\rangle_{g_1}\\
&+{}_{f_1}\left\langle\frac{T}{2},\boldsymbol{x}\left|\frac{i}{i\partial_t-H}\right|0,-\boldsymbol{R}\right\rangle_{\gamma\ \delta}\cdot\left\langle z_0,\boldsymbol{z}-\boldsymbol{R}\left|\frac{i}{i\partial_t-H}\right|z_0',\boldsymbol{z}'\right\rangle_{\alpha\ \beta}\cdot\left\langle z_0',\boldsymbol{z}'\left|\frac{i}{i\partial_t-H}\right|-\frac{T}{2},\boldsymbol{y}\right\rangle_{g_1}\\
&-{}_{f_1}\left\langle\frac{T}{2},\boldsymbol{x}\left|\frac{i}{i\partial_t-H}\right|-\frac{T}{2},\boldsymbol{y}\right\rangle_{g_1}\cdot\left\langle z_0,\boldsymbol{z}-\boldsymbol{R}\left|\frac{i}{i\partial_t-H}\right|z_0',\boldsymbol{z}'\right\rangle_{\alpha\ \beta}\cdot\left\langle z_0',\boldsymbol{z}'\left|\frac{i}{i\partial_t-H}\right|0,-\boldsymbol{R}\right\rangle_{\gamma}\Bigg]+iz_0\frac{1}{2}\{\Omega,\tilde{O}_a\}_{\gamma\delta}\\
&\times\Bigg[{}_{f_1}\left\langle\frac{T}{2},\boldsymbol{x}\left|\frac{i}{i\partial_t-H}\right|0,-\boldsymbol{R}\right\rangle_{\gamma\ \delta}\cdot\left\langle z_0,\boldsymbol{z}-\boldsymbol{R}\left|\frac{i}{i\partial_t-H}\right|-\frac{T}{2},\boldsymbol{y}\right\rangle_{g_1}\\
&-{}_{\delta}\left\langle z_0,\boldsymbol{z}-\boldsymbol{R}\left|\frac{i}{i\partial_t-H}\right|0,-\boldsymbol{R}\right\rangle_{\gamma}\cdot{}_{f_1}\left\langle\frac{T}{2},\boldsymbol{x}\left|\frac{i}{i\partial_t-H}\right|-\frac{T}{2},\boldsymbol{y}\right\rangle_{g_1}\Bigg]\Bigg\}\\
&\times\prod_{j=2}^{N_c}\left[{}_{f_j}\left\langle\frac{T}{2},\boldsymbol{x}\left|\frac{i}{i\partial_t-H}\right|-\frac{T}{2},\boldsymbol{y}\right\rangle_{g_j}\right]\cdot\exp\left[N_c\mathrm{Sp}\log(i\partial_t-H)+i\frac{I}{2}\int\Omega_a^2dt\right].
\end{aligned}
\tag{42}
$$

Let us first discuss the leading $O(\Omega^0)$ term. As usual [4,5], we introduce the eigenstates $|m\rangle$ and the associated eigenenergies E_m of the static Dirac Hamiltonian H, satisfying

$$H|m\rangle=E_m|m\rangle. \tag{43}$$

This enables us to write down a spectral representation of the single quark Green function as follows:

$$
\begin{aligned}
&{}_\alpha\left\langle\boldsymbol{x},t\left|\frac{i}{i\partial_t-H}\right|\boldsymbol{x}',t'\right\rangle_\beta\\
&=\theta(t-t')\sum_{m>0}e^{-iE_m(t-t')}{}_\alpha\langle\boldsymbol{x}|m\rangle\langle m|\boldsymbol{x}'\rangle_\beta\\
&\quad-\theta(t'-t)\sum_{m<0}e^{-iE_m(t-t')}{}_\alpha\langle\boldsymbol{x}|m\rangle\langle m|\boldsymbol{x}'\rangle_\beta.
\end{aligned}
\tag{44}
$$

Using this equation together with the relation

$$\langle\boldsymbol{z}-\boldsymbol{R}|=\langle-\boldsymbol{R}|e^{i\boldsymbol{p}\cdot\boldsymbol{z}}, \tag{45}$$

we can perform the integration over $\boldsymbol{R}$ in Eq. (41). The resultant expression is then put into Eq. (18) to carry out the integration over z_0. We then arrive at a formula, which provides us with a theoretical basis for evaluating the zeroth order contributions in Ω to quark distribution functions of the nucleon:

$$q(x;\Omega^0)=\int\Psi^{(J)*}_{J_3T_3}[\xi_A]O^{(0)}[\xi_A]\Psi^{(J)}_{J_3T_3}[\xi_A]d\xi_A, \tag{46}$$

where

$$\Psi^{(J)}_{J_3T_3}[\xi_A]=\sqrt{\frac{2J+1}{8\pi^2}}(-1)^{T+T_3}D^{(J)}_{-T_3J_3}(\xi_A), \tag{47}$$

are wave functions, describing the collective rotational motion of the hedgehog soliton, while

$$O^{(0)}[\xi_A]=M_N\frac{N_c}{2}\left(\sum_{n\leqslant0}-\sum_{n>0}\right)\langle n|\tilde{O}_a\delta(xM_N-E_n-p^3)|n\rangle. \tag{48}$$

Using the identity

$$\left(\sum_{n\leqslant0}+\sum_{n>0}\right)\langle n|\tilde{O}_a\delta(xM_N-E_n-p^3)|n\rangle=0, \tag{49}$$

Eq. (48) can be expressed in either of the following two forms:

$$
\begin{aligned}
O^{(0)}[\xi_A]&=M_NN_c\sum_{n\leqslant0}\langle n|\tilde{O}_a\delta(xM_N-E_n-p^3)|n\rangle\\
&=-M_NN_c\sum_{n>0}\langle n|\tilde{O}_a\delta(xM_N-E_n-p^3)|n\rangle,
\end{aligned}
\tag{50}
$$

i.e., as a sum over the occupied states or as a sum over the nonoccupied states. As was emphasized in [14], it is better to use the first form for $x>0$, whereas the second form for $x<0$, for the purpose of numerical calculation.

Next we turn to the $O(\Omega^1)$ contribution. In writing down Eq. (42), we have retained the time arguments $0, z_0$ and z_0' in $A^\dagger$, A and Ω, since we have to pay attention to the time order of these collective space operators, which do not generally commute after collective quantization of the rotational zero-energy modes. In the previous paper [17], motivated by the physical picture that the time-scale of deep inelastic-scattering processes is much shorter than that of collective rotational motion of the soliton, we dropped special time-order diagrams in which the Coriolis coupling Ω between the collective rotational motion and the intrinsic quark motion operates in the time interval between z_0 and 0. However, this procedure was criticized by Pobylitsa *et al.* in a recent paper [20]. According to the them, there is little reason to assume approximate degeneracy of 0 and z_0 in $A^\dagger(0)O_aA(z_0)$, since the deep-inelastic scattering processes are not necessarily short distance phenomena. Taking this nonlocality in time arguments more seriously, one should retain all the possible time-order diagrams. In doing so, we must pay attention to the time order of collective space operators A and Ω. By ordering these operators according to their time orders, we are led to the replacement

$$\begin{aligned}
&\Omega_{\alpha\beta}(z_0')(A^\dagger(0)O_aA(z_0))_{\gamma\delta}\\
&\quad\rightarrow[\theta(z_0',0,z_0)+\theta(z_0',z_0,0)]\Omega_{\alpha\beta}\tilde{O}_{\gamma\delta}\\
&\qquad+[\theta(0,z_0,z_0')+\theta(z_0,0,z_0')]\tilde{O}_{\gamma\delta}\Omega_{\alpha\beta}\\
&\qquad+\theta(0,z_0',z_0)(O_a)_{\gamma'\delta'}A^\dagger_{\gamma\gamma'}\Omega_{\alpha\beta}A_{\delta'\delta}\\
&\qquad+\theta(z_0,z_0',0)(O_a)_{\gamma'\delta'}A_{\delta'\delta}\Omega_{\alpha\beta}A^\dagger_{\gamma\gamma'}. \qquad (51)
\end{aligned}$$

Here the third and the fourth terms are new ones discarded in the treatment of [17]. In order to handle these somewhat peculiar terms, we first recall the rule of collective quantization:

$$\Omega=\frac{1}{2}\Omega_a\tau_a\rightarrow\frac{1}{2I}J_a\tau_a, \qquad (52)$$

where J_a is the total angular momentum operator satisfying the commutation relations (CR) as follows:

$$[J_a,J_b]=i\epsilon_{abc}J_c, \qquad (53)$$

$$[J_a,A]=\frac{1}{2}A\tau_a, \qquad (54)$$

$$[J_a,A^\dagger]=-\frac{1}{2}\tau_aA^\dagger. \qquad (55)$$

Using these CR, one can show that

$$\begin{aligned}
(O_a)_{\gamma'\delta'}A^\dagger_{\gamma\gamma'}\Omega_{\alpha\beta}A_{\delta'\delta}&=\frac{1}{2I}(\tau_c)_{\alpha\beta}(O_a)_{\gamma'\delta'}A^\dagger_{\gamma\gamma'}J_cA_{\delta'\delta}\\
&=\frac{1}{2I}(\tau_c)_{\alpha\beta}(O_a)_{\gamma'\delta'}A^\dagger_{\gamma\gamma'}\\
&\quad\times\left[\frac{1}{2}(A\tau_c)_{\delta'\delta}+A_{\delta'\delta}J_c\right]\\
&=\frac{1}{2I}(\tau_c)_{\alpha\beta}\left[\frac{1}{2}(A^\dagger O_aA\tau_c)_{\gamma\delta}\right.\\
&\quad\left.+(A^\dagger O_aA)_{\gamma\delta}J_c\right], \qquad (56)
\end{aligned}$$

where we have used Eq. (54). Similarly, by using Eq. (55), one may obtain an alternative expression

$$\begin{aligned}
&(O_a)_{\gamma'\delta'}A^\dagger_{\gamma\gamma'}\Omega_{\alpha\beta}A_{\delta'\delta}\\
&\quad=\frac{1}{2I}(\tau_c)_{\alpha\beta}\left[\frac{1}{2}(\tau_cA^\dagger O_aA)_{\gamma\delta}+J_c(A^\dagger O_aA)_{\gamma\delta}\right]. \qquad (57)
\end{aligned}$$

In the following manipulation, we find it convenient to take an average of these two expressions as

$$\begin{aligned}
(O_a)_{\gamma'\delta'}A^\dagger_{\gamma\gamma'}\Omega_{\alpha\beta}A_{\delta'\delta}&=\frac{1}{8I}(\tau_c)_{\alpha\beta}[(A^\dagger O_aA\tau_c)_{\gamma\delta}\\
&\quad+(\tau_cA^\dagger O_aA)_{\gamma\delta}]\\
&\quad+\frac{1}{4I}(\tau_c)_{\alpha\beta}[(A^\dagger O_aA)_{\gamma\delta}J_c\\
&\quad+J_c(A^\dagger O_aA)_{\gamma\delta}]. \qquad (58)
\end{aligned}$$

Now we must treat two cases separately. The first is the case in which the operator O_a contains an isospin factor τ_a as

$$O_a=\tau_a\overline{O}. \qquad (59)$$

In this case, using the relation $A^\dagger O_aA=D_{ab}\tau_b\overline{O}$, we can rewrite as

$$\begin{aligned}
(A^\dagger O_aA\tau_c)_{\gamma\delta}+(\tau_cA^\dagger O_aA)_{\gamma\delta}&=D_{ab}((\tau_b\tau_c+\tau_c\tau_b)\overline{O})_{\gamma\delta}\\
&=2D_{ac}(\overline{O})_{\gamma\delta}. \qquad (60)
\end{aligned}$$

On the other hand, if O_a contains no isospin factor as

$$O_a=\overline{O}, \qquad (61)$$

we obtain

$$(A^\dagger O_aA\tau_c)_{\gamma\delta}+(\tau_cA^\dagger O_aA)_{\gamma\delta}=2(\tau_c\overline{O})_{\gamma\delta}. \qquad (62)$$

Unifying the two cases, we can then write as

$$(O_a)_{\gamma'\delta'}A^{\dagger}_{\gamma\gamma'}\Omega_{\alpha\beta}A_{\delta'\delta}=\frac{1}{4I}(\tau_c)_{\alpha\beta}\begin{Bmatrix} D_{ac}\overline{O}_{\gamma\delta} \\ (\tau_c\overline{O})_{\gamma\delta}\end{Bmatrix} + \frac{1}{2}\{\Omega_{\alpha\beta},(A^{\dagger}O_aA)_{\gamma\delta}\}_+ . \tag{63}$$

$$(O_a)_{\gamma'\delta'}A_{\delta'\delta}\Omega_{\alpha\beta}A^{\dagger}_{\gamma\gamma'}=-\frac{1}{4I}(\tau_c)_{\alpha\beta}\begin{Bmatrix} D_{ac}\overline{O}_{\gamma\delta} \\ (\tau_c\overline{O})_{\gamma\delta}\end{Bmatrix} + \frac{1}{2}\{\Omega_{\alpha\beta},(A^{\dagger}O_aA)_{\gamma\delta}\}_+ . \tag{64}$$

A similar manipulation for the fourth term in Eq. (51) leads to

Retaining all these possible time order diagrams, the $O(\Omega^1)$ contribution to the distribution function now becomes

$$\begin{aligned}
\langle N(\boldsymbol{P})|\psi^{\dagger}(z)O_a\psi(0)|N(\boldsymbol{P})\rangle^{\Omega^1}=&\frac{1}{Z}\tilde{\Gamma}^{\{f\}}\tilde{\Gamma}^{\{g\}^{\dagger}}N_c\int d^3x d^3y e^{-i\boldsymbol{P}\cdot\boldsymbol{x}}e^{i\boldsymbol{P}\cdot\boldsymbol{y}}\int d^3R\int \mathcal{D}A \\
&\times\Bigg\{ i\int d^3z'dz_0'\Bigg([\theta(z_0',0,z_0)+\theta(z_0',z_0,0)]\Omega_{\alpha\beta}(\tilde{O}_a)_{\gamma\delta}+[\theta(0,z_0,z_0')+\theta(z_0,0,z_0')] \\
&\times(\tilde{O}_a)_{\gamma\delta}\Omega_{\alpha\beta}+\theta(0,z_0',z_0)\left[\frac{1}{2}\{\Omega_{\alpha\beta},(\tilde{O}_a)_{\gamma\delta}\}_+ +\frac{1}{4I}(\tau_c)_{\alpha\beta}\begin{Bmatrix} D_{ac}\overline{O}_{\gamma\delta} \\ (\tau_c\overline{O})_{\gamma\delta}\end{Bmatrix}\right]+\theta(z_0,z_0',0) \\
&\times\left[\frac{1}{2}\{\Omega_{\alpha\beta},(\tilde{O}_a)_{\gamma\delta}\}_+ -\frac{1}{4I}(\tau_c)_{\alpha\beta}\begin{Bmatrix} D_{ac}\overline{O}_{\gamma\delta} \\ (\tau_c\overline{O})_{\gamma\delta}\end{Bmatrix}\right]\Bigg) \\
&\times\Bigg[{}_{f_1}\left\langle\frac{T}{2},\boldsymbol{x}\left|\frac{i}{i\partial_t-H}\right|z_0',\boldsymbol{z}'\right\rangle_{\alpha\ \beta}\cdot\left\langle z_0',\boldsymbol{z}'\left|\frac{i}{i\partial_t-H}\right|0,-\boldsymbol{R}\right\rangle_{\gamma\ \delta}\cdot\left\langle z_0,\boldsymbol{z}-\boldsymbol{R}\left|\frac{i}{i\partial_t-H}\right|-\frac{T}{2},\boldsymbol{y}\right\rangle_{g_1} \\
&+{}_{f_1}\left\langle\frac{T}{2},\boldsymbol{x}\left|\frac{i}{i\partial_t-H}\right|0,-\boldsymbol{R}\right\rangle_{\gamma\ \delta}\cdot\left\langle z_0,\boldsymbol{z}-\boldsymbol{R}\left|\frac{i}{i\partial_t-H}\right|z_0',\boldsymbol{z}'\right\rangle_{\alpha\ \beta}\cdot\left\langle z_0',\boldsymbol{z}'\left|\frac{i}{i\partial_t-H}\right|-\frac{T}{2},\boldsymbol{y}\right\rangle_{g_1} \\
&-{}_{f_1}\left\langle\frac{T}{2},\boldsymbol{x}\left|\frac{i}{i\partial_t-H}\right|-\frac{T}{2},\boldsymbol{y}\right\rangle_{g_1\ \delta}\cdot\left\langle z_0,\boldsymbol{z}-\boldsymbol{R}\left|\frac{i}{i\partial_t-H}\right|z_0',\boldsymbol{z}'\right\rangle_{\alpha\ \beta}\cdot\left\langle z_0',\boldsymbol{z}'\left|\frac{i}{i\partial_t-H}\right|0,-\boldsymbol{R}\right\rangle_{\gamma}\Bigg] \\
&+iz_0\frac{1}{2}\{\Omega,\tilde{O}_a\}_{\gamma\delta}\Bigg[{}_{f_1}\left\langle\frac{T}{2},\boldsymbol{x}\left|\frac{i}{i\partial_t-H}\right|0,-\boldsymbol{R}\right\rangle_{\gamma\ \delta}\cdot\left\langle z_0,\boldsymbol{z}-\boldsymbol{R}\left|\frac{i}{i\partial_t-H}\right|-\frac{T}{2},\boldsymbol{y}\right\rangle_{g_1} \\
&-{}_{\delta}\left\langle z_0,\boldsymbol{z}-\boldsymbol{R}\left|\frac{i}{i\partial_t-H}\right|0,-\boldsymbol{R}\right\rangle_{\gamma\ f_1}\cdot\left\langle\frac{T}{2},\boldsymbol{x}\left|\frac{i}{i\partial_t-H}\right|-\frac{T}{2},\boldsymbol{y}\right\rangle_{g_1}\Bigg]\Bigg\} \\
&\times\prod_{j=2}^{N_c}\left[{}_{f_j}\left\langle\frac{T}{2},\boldsymbol{x}\left|\frac{i}{i\partial_t-H}\right|-\frac{T}{2},\boldsymbol{y}\right\rangle_{g_j}\right]\cdot\exp\left[N_c\mathrm{Sp}\log(i\partial_t-H)+i\frac{I}{2}\int\Omega_a^2dt\right].
\end{aligned} \tag{65}$$

After stating all the delicacies inherent in the structure function problem, we can now proceed in the same way as [17] and [24]. Using the spectral representation of the single quark Green function (44) together with the relation (45), we can perform the integration over $\boldsymbol{R},\boldsymbol{z}'$, and z_0'. The resultant expression is then put into Eq. (18) to carry out the integration over z_0. We then arrive at a formula, which gives a theoretical basis for evaluating the $O(\Omega^1)$ contributions to quark distribution functions of the nucleon

$$q(x;\Omega^1)=\int\Psi^{(J)*}_{J_3T_3}[\xi_A]O^{(1)}[\xi_A]\Psi^{(J)}_{J_3T_3}[\xi_A]d\xi_A , \tag{66}$$

where

$$O^{(1)}[\xi_A]=O_A^{(1)}+O_B^{(1)}+O_{B'}^{(1)}+O_C^{(1)}, \tag{67}$$

with

$$O_A^{(1)}=M_N\frac{N_c}{2}\sum_{m>0,n\leqslant 0}\frac{1}{E_m-E_n}[\langle n|\tilde{O}_a(\delta_n+\delta_m)|m\rangle\langle m|\Omega|n\rangle+\langle n|\Omega|m\rangle\langle m|\tilde{O}_a(\delta_n+\delta_m)|n\rangle], \tag{68}$$

$$O_B^{(1)}=M_N\frac{N_c}{4}\left(\sum_{m\leqslant 0,n\leqslant 0}-\sum_{n>0,m>0}\right)\frac{1}{E_m-E_n}[\langle n|\tilde{O}_a(\delta_n-\delta_m)|m\rangle\langle m|\Omega|n\rangle+\langle n|\Omega|m\rangle\langle m|\tilde{O}_a(\delta_n-\delta_m)|n\rangle], \tag{69}$$

$$O_{B'}^{(1)}=M_N\frac{N_c}{8I}\left(\sum_{m\leqslant 0,n\leqslant 0}-\sum_{n>0,m>0}\right)\frac{1}{E_m-E_n}\langle n|\tau_c|m\rangle\langle m|\begin{Bmatrix}D_{ac}\overline{O}\\ \tau_c\overline{O}\end{Bmatrix}(\delta_n-\delta_m)|n\rangle, \tag{70}$$

$$O_C^{(1)}=\frac{d}{dx}\frac{N_c}{4}\left(\sum_{n\leqslant 0}-\sum_{n>0}\right)\langle n|\{\tilde{O}_a,\Omega\}\delta_n|n\rangle. \tag{71}$$

In the above equations, we have used the notation

$$\delta_m\equiv\delta(xM_N-E_m-p^3),\ \text{ and }\ \delta_n\equiv\delta(xM_N-E_n-p^3) \tag{72}$$

for saving space. Here $O_A^{(1)}$ is the contribution from the diagram in which z_0' is later (or earlier) than both of 0 and z_0. As was emphasized in [17], this term contains transitions between the occupied and nonoccupied single quark levels so that it is not in conflict with the Pauli principle. On the other hand, $O_B^{(1)}$ and $O_{B'}^{(1)}$ are the contributions from diagrams in which z_0' lies between 0 and z_0. Although these terms appear to contain Pauli-violating transitions between the occupied levels themselves or the nonoccupied ones, we take here the viewpoint advocated in [20] that there is no compulsory reason to drop them since we are here dealing with operators which are nonlocal in time. Finally, $O_C^{(1)}$ is the $O(\Omega^1)$ contribution resulting from the nonlocality of the operator $A^\dagger(0)O_aA(z_0)$, i.e., the second term of Eq. (38). In deriving $O_C^{(1)}$, use has been made of the identity

$$\frac{1}{2\pi}\int_{-\infty}^{\infty}dz_0 iz_0 e^{i(xM_N-E_n-p^3)z_0}=\frac{1}{M_N}\frac{\partial}{\partial x}\delta(xM_N-E_n-p^3). \tag{73}$$

As will become clear shortly, it is convenient to treat $O_A^{(1)}$ and $O_B^{(1)}$ in a combined way. To see it, first note that, after a simple change of summation indices, $O_A^{(1)}$ can be rewritten as

$$\begin{aligned}O_A^{(1)}=M_N\frac{N_c}{2}\Bigg\{&\sum_{m>0,n\leqslant 0}\frac{1}{E_m-E_n}[\langle n|\tilde{O}_a\delta_n|m\rangle\langle m|\Omega|n\rangle+\langle n|\Omega|m\rangle\langle m|\tilde{O}_a\delta_n|n\rangle]\\ &-\sum_{m\leqslant 0,n>0}\frac{1}{E_m-E_n}[\langle m|\tilde{O}_a\delta_n|n\rangle\langle n|\Omega|m\rangle+\langle m|\Omega|n\rangle\langle n|\tilde{O}_a\delta_n|m\rangle]\Bigg\}.\end{aligned} \tag{74}$$

From now on, we treat the two cases separately. First, assume that the relevant operator O_a contains an isospin factor τ_a in such a form as $O_a=\tau_a\overline{O}$. In this case, in view of the relations $\tilde{O}_a=A^\dagger O_aA=D_{ab}\tau_b\overline{O}$ and $\Omega=(1/2I)J_c\tau_c$, we must carefully treat the noncommutativity of the two collective space operators D_{ab} and J_c. By keeping the order of D_{ab} and J_c, $O_A^{(1)}$ can generally be divided into two pieces [24] as

$$O_A^{(1)}=M_N\frac{N_c}{4I}\frac{1}{2}\{D_{ab},J_c\}_+\Bigg\{\sum_{m>0,n\leqslant 0}\frac{1}{E_m-E_n}[\langle n|\tau_b\overline{O}\delta_n|m\rangle\langle m|\tau_c|n\rangle+\langle n|\tau_c|m\rangle\langle m|\tau_b\overline{O}\delta_n|n\rangle]$$
$$-\sum_{m\leqslant 0,n>0}\frac{1}{E_m-E_n}[\langle n|\tau_b\overline{O}\delta_n|m\rangle\langle m|\tau_c|n\rangle+\langle n|\tau_c|m\rangle\langle m|\tau_b\overline{O}\delta_n|n\rangle]\Bigg\}+M_N\frac{N_c}{4I}\frac{1}{2}[D_{ab},J_c]$$
$$\times\Bigg\{\sum_{m>0,n\leqslant 0}\frac{1}{E_m-E_n}[\langle n|\tau_b\overline{O}\delta_n|m\rangle\langle m|\tau_c|n\rangle-\langle n|\tau_c|m\rangle\langle m|\tau_b\overline{O}\delta_n|n\rangle]$$
$$-\sum_{m\leqslant 0,n>0}\frac{1}{E_m-E_n}[\langle n|\tau_b\overline{O}\delta_n|m\rangle\langle m|\tau_c|n\rangle-\langle n|\tau_c|m\rangle\langle m|\tau_b\overline{O}\delta_n|n\rangle]\Bigg\}, \tag{75}$$

which contains symmetric and antisymmetric combinations of the two collective space operators D_{ab} and J_c. On the other hand, it can be easily verified that $O_B^{(1)}$ term contains symmetric combination only:

$$O_B^{(1)}=M_N\frac{N_c}{4I}\frac{1}{2}\{D_{ab},J_c\}_+\Bigg\{\sum_{m>0,n\leqslant 0}\frac{1}{E_m-E_n}[\langle n|\tau_b\overline{O}\delta_n|m\rangle\langle m|\tau_c|n\rangle+\langle n|\tau_c|m\rangle\langle m|\tau_b\overline{O}\delta_n|n\rangle]$$
$$-\sum_{m\leqslant 0,n>0}\frac{1}{E_m-E_n}[\langle n|\tau_b\overline{O}\delta_n|m\rangle\langle m|\tau_c|n\rangle+\langle n|\tau_c|m\rangle\langle m|\tau_b\overline{O}\delta_n|n\rangle]\Bigg\}. \tag{76}$$

Combining $O_A^{(1)}$ and $O_B^{(1)}$ terms, we then obtain for the isovector case

$$O_A^{(1)}+O_B^{(1)}=O_{\{A,B\}}^{(1)}+O_{[A,B]}^{(1)}, \tag{77}$$

where

$$O_{\{A,B\}}^{(1)}=M_N\frac{N_c}{4I}\frac{1}{2}\{D_{ab},J_c\}_+\Bigg(\sum_{m>0,n\leqslant 0}-\sum_{m\leqslant 0,n>0}+\sum_{m\leqslant 0,n\leqslant 0}-\sum_{m>0,n>0}\Bigg)$$
$$\times\frac{1}{E_m-E_n}[\langle n|\tau_b\overline{O}\delta_n|m\rangle\langle m|\tau_c|n\rangle+\langle n|\tau_c|m\rangle\langle m|\tau_b\overline{O}\delta_n|n\rangle] \tag{78}$$

$$O_{[A,B]}^{(1)}=M_N\frac{N_c}{4I}\frac{1}{2}[D_{ab},J_c]\Bigg(\sum_{m>0,n\leqslant 0}+\sum_{m\leqslant 0,n>0}\Bigg)\frac{1}{E_m-E_n}[\langle n|\tau_b\overline{O}\delta_n|m\rangle\langle m|\tau_c|n\rangle-\langle n|\tau_c|m\rangle\langle m|\tau_b\overline{O}\delta_n|n\rangle]. \tag{79}$$

The situation is much simpler for isoscalar operators $O_a=\overline{O}$. Since $\tilde{O}_a=A^\dagger O_a A=A^\dagger\overline{O}A=\overline{O}$, we have only to replace both of D_{ab} and τ_b by 1 in the above manipulation, thereby leading to

$$O_{\{A,B\}}^{(1)}=M_N\frac{N_c}{4I}J_c\Bigg(\sum_{m>0,n\leqslant 0}-\sum_{m\leqslant 0,n>0}+\sum_{m\leqslant 0,n\leqslant 0}-\sum_{m>0,n>0}\Bigg)\frac{1}{E_m-E_n}[\langle n|\overline{O}\delta_n|m\rangle\langle m|\tau_c|n\rangle+\langle n|\tau_c|m\rangle\langle m|\overline{O}\delta_n|n\rangle], \tag{80}$$

$$O_{[A,B]}^{(1)}=0. \tag{81}$$

One notices that only the symmetric combination of the matrix elements survives for this isoscalar case. This should be contrasted to the isovector case in which either of the symmetric part or the antisymmetric part survives, depending on the symmetry property of the relevant single quark matrix elements appearing in Eqs. (78) and (79). As we shall discuss later, the symmetric part contributes to the isoscalar polarized distribution function $\Delta u(x)+\Delta d(x)$ and $\delta u(x)+\delta d(x)$ at the $O(\Omega^1)$, whereas the antisymmetric part plays an important role in the $O(\Omega^1)$ term of the isovector polarized distribution functions $\Delta u(x)-\Delta d(x)$ or $\delta u(x)-\delta d(x)$ [24].

Now we shall investigate the case of our interest in more detail for obtaining explicit formulas, which can be used for numerical calculation of polarized distribution functions of the nucleon.

A. $\Delta u(x)+\Delta d(x)$

The relevant operator in this case is

$$\tilde{O}_a=A^\dagger(1+\gamma^0\gamma^3)\gamma_5 A=(1+\gamma^0\gamma^3)\gamma^5. \tag{82}$$

Since the $O(\Omega^0)$ contribution to $\Delta u(x)+\Delta d(x)$ vanishes due to the hedgehog symmetry, the leading contribution to this distribution function arises from the $O(\Omega^1)$ terms. Due to the symmetry property of the relevant single quark matrix elements, only the symmetric combination of $O_A^{(1)}+O_B^{(1)}$ survives. The total $O(\Omega^1)$ term therefore consists of three pieces, $O_{\{A,B\}}^{(1)}$, $O_{B'}$ and $O_C^{(1)}$. Using the general formulas obtained so far, the contributions of these three terms to $\Delta u(x)+\Delta d(x)$ are given as

$$[\Delta u(x)+\Delta d(x)]_{\{A,B\}}^{(1)}=\langle J_3\rangle_{p\uparrow}\cdot M_N\frac{N_c}{4I}\left(\sum_{m=all,n\leqslant 0}-\sum_{m=all,n>0}\right)\frac{1}{E_m-E_n}$$
$$\times[\langle n|(1+\gamma^0\gamma^3)\gamma_5\delta_n|m\rangle\langle m|\tau_3|n\rangle+\langle n|\tau_3|m\rangle\langle m|(1+\gamma^0\gamma^3)\gamma_5\delta_n|n\rangle], \tag{83}$$

$$[\Delta u(x)+\Delta d(x)]_{B'}^{(1)}=\langle 1\rangle_{p\uparrow}\cdot M_N\frac{N_c}{8I}\left(\sum_{m\leqslant 0,n\leqslant 0}-\sum_{m>,n>0}\right)\frac{1}{E_m-E_n}\langle n|\tau_c|m\rangle\langle m|\tau_c(1+\gamma^0\gamma^3)\gamma_5(\delta_n-\delta_m)|n\rangle, \tag{84}$$

$$[\Delta u(x)+\Delta d(x)]_C^{(1)}=\langle J_3\rangle_{p\uparrow}\cdot\frac{d}{dx}M_N\frac{N_c}{4I}\left(\sum_{n\leqslant 0}-\sum_{n>0}\right)\langle n|\tau_3(1+\gamma^0\gamma^3)\gamma_5\delta_n|n\rangle. \tag{85}$$

In the above equations, $\langle\mathcal{O}\rangle_{p\uparrow}$ denotes a matrix element of a collective space operator $\mathcal{O}$ with respect to the proton in the spin up state along the z-axis, i.e.,

$$\langle\mathcal{O}\rangle_{p\uparrow}=\int\Psi_{(1/2)(1/2)}^{(1/2)}[\xi_A]\mathcal{O}\Psi_{(1/2)(1/2)}^{(1/2)}[\xi_A]d\xi_A=\langle p,S_z=1/2|\mathcal{O}|p,S_z=1/2\rangle. \tag{86}$$

In deriving Eq. (83), we have used the relation

$$\langle\{\tilde{O}_a,\Omega\}_+\rangle_{p\uparrow}=\left\langle\left\{(1+\gamma^0\gamma^3)\gamma_5,\frac{1}{2I}J_c\tau_c\right\}_+\right\rangle_{p\uparrow}=\frac{1}{I}\langle J_3\rangle_{p\uparrow}\cdot\tau_3(1+\gamma^0\gamma^3)\gamma_5. \tag{87}$$

One may notice that the collective space operator contained in the term $[\Delta u(x)+\Delta d(x)]_{B'}^{(1)}$ is 1 and it is different from J_3 contained in other two terms. The appearance of this term seems to be inconsistent, since it does not change sign in contrast to the other two terms when the direction of the proton spin is reversed. Fortunately, it can be shown that this potentially dangerous term vanishes identically due to the symmetry of the double sum of the single quark matrix element:

$$[\Delta u(x)+\Delta d(x)]_{B'}^{(1)}=0. \tag{88}$$

We are then left with the two terms, i.e., $[\Delta u(x)+\Delta d(x)]_{\{A,B\}}^{(1)}$ and $[\Delta u(x)+\Delta d(x)]_C^{(1)}$, which both have required state dependence. For the purpose of numerical calculation, it is convenient to rewrite the above two terms slightly further. A key relation in this manipulation is the following identity:

$$\left(\sum_{m=all,n\leqslant 0}+\sum_{m=all,n>0}\right)\frac{1}{E_m-E_n}[\langle n|(1+\gamma^0\gamma^3)\gamma_5\delta_n|m\rangle\langle m|\tau_3|n\rangle+\langle n|\tau_3|m\rangle\langle m|(1+\gamma^0\gamma^3)\gamma_5\delta_n|n\rangle]=0. \tag{89}$$

That this identity holds can be seen as follows. We first point out that, after separating from the double sum of Eq. (89) the sum over terms with $E_m=E_n$, we can rewrite it as

$$0=2\sum_{\substack{m=all,n=all\\(E_m\neq E_n)}}\frac{1}{E_m-E_n}\langle n|\tau_3|m\rangle\langle m|(1+\gamma^0\gamma^3)\gamma_5\delta_n|n\rangle+\frac{1}{M_N}\frac{d}{dx}\sum_{\substack{m=all,n=all\\(E_m=E_n)}}\langle n|\tau_3|m\rangle\langle m|(1+\gamma^0\gamma^3)\gamma_5\delta_n|n\rangle. \tag{90}$$

This essentially coincides with Eq. (A18) given in Appendix A of [20] except that the operators τ_a and $\tau_a(1+\gamma^0\gamma^3)$ there are replaced here by τ_3 and $(1+\gamma^0\gamma^3)\gamma_5$, respectively. The proof given in Appendix of [20] then holds without any essential modification. (For assurance, we shall later try to check to what extent this identity holds in our numerical calculation.) Assuming the validity of the above identity (89), $[\Delta u(x)+\Delta d(x)]_{\{A,B\}}^{(1)}$ can be expressed in either of the following two forms:

$$[\Delta u(x)+\Delta d(x)]^{(1)}_{\{A,B\}}=\langle 2J_3\rangle_{p\uparrow}\cdot M_N\frac{N_c}{4I}\sum_{m=all,n\leqslant 0}\frac{1}{E_m-E_n}$$
$$\times[\langle n|(1+\gamma^0\gamma^3)\gamma_5\delta_n|m\rangle\langle m|\tau_3|n\rangle+\langle n|\tau_3|m\rangle\langle m|(1+\gamma^0\gamma^3)\gamma_5\delta_n|n\rangle]$$
$$=-\langle 2J_3\rangle_{p\uparrow}\cdot M_N\frac{N_c}{4I}\sum_{m=all,n>0}\frac{1}{E_m-E_n}$$
$$\times[\langle n|(1+\gamma^0\gamma^3)\gamma_5\delta_n|m\rangle\langle m|\tau_3|n\rangle+\langle n|\tau_3|m\rangle\langle m|(1+\gamma^0\gamma^3)\gamma_5\delta_n|n\rangle]. \quad (91)$$

As advocated in [20], it is convenient to use the first expression given as a sum over the occupied states for the numerical calculation of distribution functions in the region $x>0$, while to use the second one given as sum over the nonoccupied states when $x<0$, since one can thus avoid vacuum subtraction, i.e., subtraction of the corresponding sums over vacuum levels (with $U=1$). Following [20], we also separate the $E_m=E_n$ contribution from the above sum over the single quark levels. This can be done by noting the identities

$$\sum_{m\leqslant 0,n\leqslant 0}\frac{1}{E_m-E_n}[\langle n|(1+\gamma^0\gamma^3)\gamma_5\delta_n|m\rangle\langle m|\tau_3|n\rangle+\langle n|\tau_3|m\rangle\langle m|(1+\gamma^0\gamma^3)\gamma_5\delta_n|n\rangle]$$
$$=\frac{1}{2}\sum_{m\leqslant 0,n\leqslant 0}\frac{1}{E_m-E_n}[\langle n|(1+\gamma^0\gamma^3)\gamma_5(\delta_n-\delta_m)|m\rangle\langle m|\tau_3|n\rangle+\langle n|\tau_3|m\rangle\langle m|(1+\gamma^0\gamma^3)\gamma_5(\delta_n-\delta_m)|n\rangle], \quad (92)$$

and

$$\lim_{E_m\to E_n}\frac{\delta(xM_N-E_n-p^3)-\delta(xM_N-E_m-p^3)}{E_m-E_n}=\delta'(xM_N-E_n-p^3)=\frac{1}{M_N}\frac{d}{dx}\delta(xM_N-E_n-p^3). \quad (93)$$

From Eq. (91), we can then readily obtain

$$[\Delta u(x)+\Delta d(x)]^{(1)}_{\{A,B\}}=\langle 2J_3\rangle_{p\uparrow}\cdot M_N\frac{N_c}{4I}\sum_{\substack{m=all,n\leqslant 0\\(E_m\neq E_n)}}\frac{1}{E_m-E_n}$$
$$\times[\langle n|(1+\gamma^0\gamma^3)\gamma_5\delta_n|m\rangle\langle m|\tau_3|n\rangle+\langle n|\tau_3|m\rangle\langle m|(1+\gamma^0\gamma^3)\gamma_5\delta_n|n\rangle]+\langle J_3\rangle_{p\uparrow}\cdot\frac{d}{dx}\frac{N_c}{8I}$$
$$\times\sum_{\substack{m\leqslant 0,n\leqslant 0\\(E_m=E_n)}}[\langle n|(1+\gamma^0\gamma^3)\gamma_5\delta_n|m\rangle\langle m|\tau_3|n\rangle+\langle n|\tau_3|m\rangle\langle m|(1+\gamma^0\gamma^3)\gamma_5\delta_n|n\rangle], \quad (94)$$

and a corresponding expression given as sums over non-occupied levels. The remaining term $[\Delta u(x)+\Delta d(x)]^{(1)}_C$ can similarly be expressed in either of the two equivalent forms as

$$[\Delta u(x)+\Delta d(x)]^{(1)}_C=\langle 2J_3\rangle_{p\uparrow}\cdot\frac{d}{dx}\frac{N_c}{4I}\sum_{n\leqslant 0}\langle n|\tau_3(1+\gamma^0\gamma^3)\gamma_5\delta_n|n\rangle$$
$$=-\langle 2J_3\rangle_{p\uparrow}\cdot\frac{d}{dx}\frac{N_c}{4I}\sum_{n>0}\langle n|\tau_3(1+\gamma^0\gamma^3)\gamma_5\delta_n|n\rangle. \quad (95)$$

Inserting the complete set of single quark states into the first expression and separating the $E_m\neq E_n$ and $E_m=E_n$ terms in this sum, we obtain

$$[\Delta u(x)+\Delta d(x)]^{(1)}_C=\langle 2J_3\rangle_{p\uparrow}\cdot\frac{d}{dx}\frac{N_c}{4I}\sum_{\substack{m=all,n\leqslant 0\\(E_m\neq E_n)}}\langle n|\tau_3|m\rangle\langle m|(1+\gamma^0\gamma^3)\gamma_5\delta_n|n\rangle$$
$$+\langle 2J_3\rangle_{p\uparrow}\cdot\frac{d}{dx}\frac{N_c}{4I}\sum_{\substack{m\leqslant 0,n\leqslant 0\\(E_m=E_n)}}\langle n|\tau_3|m\rangle\langle m|(1+\gamma^0\gamma^3)\gamma_5\delta_n|n\rangle, \quad (96)$$

and a corresponding expression given as sums over nonoccupied states. Just as argued in [20] for the case of the unpolarized distribution function $u(x)-d(x)$, $E_m=E_n$ contribution in the double sums in $[\Delta u(x)+\Delta d(x)]^{(1)}_{\{A,B\}}$ and $[\Delta u(x)+\Delta d(x)]^{(1)}_{C}$ precisely cancel each other. After regrouping the terms in such a way that this cancellation occurs at the level of analytical expressions, the $O(\Omega^1)$ contribution to the distribution function $\Delta u(x)+\Delta d(x)$ can finally be written in the following form:

$$[\Delta u(x)+\Delta d(x)]^{(1)}=[\Delta u(x)+\Delta d(x)]^{(1)}_{\{A,B\}'}+[\Delta u(x)+\Delta d(x)]^{(1)}_{C'} \tag{97}$$

where

$$[\Delta u(x)+\Delta d(x)]^{(1)}_{\{A,B\}'}=\langle 2J_3\rangle_{p\uparrow}\cdot M_N\frac{N_c}{2I}\sum_{\substack{m=all,n\leqslant 0\\(E_m\neq E_n)}}\frac{1}{E_m-E_n}\langle n|(1+\gamma^0\gamma^3)\gamma_5\delta_n|m\rangle\langle m|\tau_3|n\rangle, \tag{98}$$

$$=-\langle 2J_3\rangle_{p\uparrow}\cdot M_N\frac{N_c}{2I}\sum_{\substack{m=all,n>0\\(E_m\neq E_n)}}\frac{1}{E_m-E_n}\langle n|(1+\gamma^0\gamma^3)\gamma_5\delta_n|m\rangle\langle m|\tau_3|n\rangle, \tag{99}$$

and

$$[\Delta u(x)+\Delta d(x)]^{(1)}_{C'}=\langle 2J_3\rangle_{p\uparrow}\cdot\frac{d}{dx}\frac{N_c}{4I}\sum_{\substack{m=all,n\leqslant 0\\(E_m\neq E_n)}}\langle n|\tau_3|m\rangle\langle m|(1+\gamma^0\gamma^3)\gamma_5\delta_n|n\rangle, \tag{100}$$

$$=-\langle 2J_3\rangle_{p\uparrow}\cdot\frac{d}{dx}\frac{N_c}{4I}\sum_{\substack{m=all,n>0\\(E_m\neq E_n)}}\langle n|\tau_3|m\rangle\langle m|(1+\gamma^0\gamma^3)\gamma_5\delta_n|n\rangle. \tag{101}$$

These expressions will be used in the numerical calculation.

B. $\Delta u(x)-\Delta d(x)$

The relevant operator for the isovector longitudinally polarized distribution function is

$$\tilde{O}_{a=3}=A^\dagger\tau_3(1+\gamma^0\gamma^3)\gamma_5 A=D_{3b}\tau_b(1+\gamma^0\gamma^3)\gamma_5. \tag{102}$$

The main contribution to this distribution function comes from the 0th order term in Ω. A simple manipulation gives

$$[\Delta u(x)-\Delta d(x)]^{(0)}=\langle D_{33}\rangle_{p\uparrow}\cdot M_N N_c\sum_{n\leqslant 0}\langle n|\tau_3(1+\gamma^0\gamma^3)\gamma_5\delta_n|n\rangle$$

$$=-\langle D_{33}\rangle_{p\uparrow}\cdot M_N N_c\sum_{n>0}\langle n|\tau_3(1+\gamma^0\gamma^3)\gamma_5\delta_n|n\rangle. \tag{103}$$

The $O(\Omega^1)$ contribution to $\Delta u(x)-\Delta d(x)$ is far more complicated. It generally consists of 4 terms, $O^{(1)}_A$, $O^{(1)}_B$, $O^{(1)}_{B'}$ and $O^{(1)}_C$. As was already mentioned, the symmetric part of the sum of $O^{(1)}_A$ and $O^{(1)}_B$ vanishes for this particular operator, owing to the symmetry of the single quark matrix elements. Using the familiar commutation relation

$$[J_c,D_{3b}]=i\epsilon_{cbe}D_{3e}, \tag{104}$$

the antisymmetric part of $O^{(1)}_A+O^{(1)}_B$ becomes

$$[\Delta u(x)-\Delta d(x)]^{(1)}_{[A,B]}=\langle D_{33}\rangle_{p\uparrow}\cdot M_N\frac{N_c}{8I}i\epsilon_{3cb}\sum_{m>0,n\leqslant 0}\frac{1}{E_m-E_n}[\langle n|\tau_c|m\rangle\langle m|\tau_b(1+\gamma^0\gamma^3)\gamma_5(\delta_n+\delta_m)|n\rangle$$
$$-\langle n|\tau_b(1+\gamma^0\gamma^3)\gamma_5(\delta_n+\delta_m)|m\rangle\langle m|\tau_c|n\rangle]$$
$$=-\langle D_{33}\rangle_{p\uparrow}\cdot M_N\frac{1}{I}\frac{N_c}{2}\sum_{m>0,n\leqslant 0}\frac{1}{E_m-E_n}\Bigg[\langle n|\tau_{+1}|m\rangle\langle n|\tau_{+1}(\gamma_5+\Sigma_3)\frac{\delta_n+\delta_m}{2}|m\rangle$$
$$-\langle n|\tau_{-1}|m\rangle\langle n|\tau_{-1}(\gamma_5+\Sigma_3)\frac{\delta_n+\delta_m}{2}|m\rangle\Bigg], \tag{105}$$

with the standard definition $\tau_\pm=\mp(\tau_1\pm i\tau_2)/\sqrt{2}$ and $\Sigma_3=\gamma^0\gamma^3\gamma_5$. Next, from Eq. (70) with the case of isovector operator, we find that

$$[\Delta u(x)-\Delta d(x)]^{(1)}_{B'}=\langle D_{33}\rangle_{p\uparrow}\cdot M_N\frac{N_c}{8I}\Bigg(\sum_{m\leqslant 0,n\leqslant 0}-\sum_{m>0,n>0}\Bigg)\frac{1}{E_m-E_n}\langle n|\tau_3|m\rangle\langle m|(1+\gamma^0\gamma^3)\gamma_5(\delta_n-\delta_m)|n\rangle. \tag{106}$$

One should notice that the state dependence of this somewhat peculiar contribution is nothing different from that of the main term, which implies that there is no reason for this term to vanish. In fact, the single quark matrix element appearing in the above double sum is essentially the same as that appearing in the expression for $[\Delta u(x)+\Delta d(x)]^{(1)}$.

The last but potentially important contribution comes from the nonlocality correction term $O^{(1)}_C$. First note that

$$\{\tilde{O}_{a=3},\Omega\}_+=\Bigg\{D_{3b}\tau_b(1+\gamma^0\gamma^3)\gamma_5,\frac{1}{2I}J_c\tau_c\Bigg\}_+$$
$$=\frac{1}{2I}\Bigg(\frac{1}{2}\{D_{3b},J_c\}_+[\tau_b(1+\gamma^0\gamma^3)\gamma_5\tau_c+\tau_c\tau_b(1+\gamma^0\gamma^3)\gamma_5]$$
$$+\frac{1}{2}[D_{3b},J_c][\tau_b(1+\gamma^0\gamma^3)\gamma_5\tau_c-\tau_c\tau_b(1+\gamma^0\gamma^3)\gamma_5]\Bigg)$$
$$=\frac{1}{2I}(\{D_{3c},J_c\}_+(1+\gamma^0\gamma^3)\gamma_5+i\epsilon_{bce}[D_{3b},J_c]\tau_e(1+\gamma^0\gamma^3)\gamma_5). \tag{107}$$

The first term of the above equation does not contribute, since

$$\sum_{n\leqslant 0}\langle n|(1+\gamma^0\gamma^3)\gamma_5\delta_n|n\rangle+\sum_{n>0}\langle n|(1+\gamma^0\gamma^3)\gamma_5\delta_n|n\rangle=0. \tag{108}$$

Simplifying the second term by using the CR (104), we finally obtain

$$[\Delta u(x)-\Delta d(x)]^{(1)}_C=-\langle D_{33}\rangle^{(1)}_{p\uparrow}\cdot\frac{d}{dx}\frac{N_c}{4I}\Bigg(\sum_{n\leqslant 0}-\sum_{n>0}\Bigg)\langle n|\tau_3(1+\gamma^0\gamma^3)\gamma^5\delta_n|n\rangle. \tag{109}$$

For the same reason as before, it is convenient to consider these term in a combined way. To this end, we first rewrite Eq. (109) by inserting a complete set of single quark states and by separating the $E_m=E_n$ contributions from the resultant double sum. The result can be expressed in two alternative forms as

$$[\Delta u(x)-\Delta d(x)]^{(1)}_C=-\langle D_{33}\rangle_{p\uparrow}\cdot\frac{d}{dx}\frac{N_c}{4I}\Bigg(\sum_{\substack{m=all,n\leqslant 0\\(E_m\neq E_n)}}+\sum_{\substack{m\leqslant 0,n\leqslant 0\\(E_m=E_n)}}\Bigg)\langle n|\tau_3|m\rangle\langle m|(1+\gamma^0\gamma^3)\gamma_5\delta_n|n\rangle$$
$$=\langle D_{33}\rangle_{p\uparrow}\cdot\frac{d}{dx}\frac{N_c}{4I}\Bigg(\sum_{\substack{m=all,n>0\\E_m\neq E_n}}+\sum_{\substack{m>0,n>0\\E_m=E_n}}\Bigg)\langle n|\tau_3|m\rangle\langle m|(1+\gamma^0\gamma^3)\gamma_5\delta_n|n\rangle. \tag{110}$$

To rewrite the B' term, we first separate $E_m=E_n$ contributions in the double sum of Eq. (105) as

$$[\Delta u(x)-\Delta d(x)]^{(1)}_{B'}=\langle D_{33}\rangle_{p\uparrow}\cdot M_N\frac{N_c}{4I}\left(\sum_{\substack{m\le 0,n\le 0\\(E_m\neq E_n)}}-\sum_{\substack{m>0,n>0\\(E_m\neq E_n)}}\right)\frac{1}{E_m-E_n}\langle n|\tau_3|m\rangle\langle m|(1+\gamma^0\gamma^3)\gamma_5\delta_n|n\rangle$$
$$+\langle D_{33}\rangle_{p\uparrow}\cdot\frac{d}{dx}\frac{N_c}{8I}\left(\sum_{\substack{m\le 0,n\le 0\\(E_m=E_n)}}-\sum_{\substack{m>0,n>0\\(E_m=E_n)}}\right)\langle n|\tau_3|m\rangle\langle m|(1+\gamma^0\gamma^3)\gamma_5\delta_n|n\rangle. \quad (111)$$

Next, we notice the identity

$$0=\sum_{\substack{m=all,n=all\\(E_m\neq E_n)}}\frac{1}{E_m-E_n}\langle n|\tau_3|m\rangle\langle m|(1+\gamma^0\gamma^3)\gamma_5\delta_n|n\rangle+\frac{1}{2M_N}\frac{d}{dx}\sum_{\substack{m=all,n=all\\(E_m=E_n)}}\langle n|\tau_3|m\rangle\langle m|(1+\gamma^0\gamma^3)\gamma_5\delta_n|n\rangle. \quad (112)$$

Using this identity, Eq. (111) can be rewritten in either of the following two forms:

$$[\Delta u(x)-\Delta d(x)]^{(1)}_{B'}=\langle D_{33}\rangle_{p\uparrow}\cdot M_N\frac{N_c}{4I}\left(2\sum_{\substack{m\le 0,n\le 0\\(E_m\neq E_n)}}+\sum_{m>0,n\le 0}+\sum_{m\le 0,n>0}\right)\frac{1}{E_m-E_n}\langle n|\tau_3|m\rangle\langle m|(1+\gamma^0\gamma^3)\gamma_5\delta_n|n\rangle$$
$$+\langle D_{33}\rangle_{p\uparrow}\cdot\frac{d}{dx}\frac{N_c}{4I}\sum_{\substack{m\le 0,n\le 0\\(E_m=E_n)}}\langle n|\tau_3|m\rangle\langle m|(1+\gamma^0\gamma^3)\gamma_5\delta_n|n\rangle$$
$$=-\langle D_{33}\rangle_{p\uparrow}\cdot M_N\frac{N_c}{4I}\left(2\sum_{\substack{m>0,n>0\\(E_m\neq E_n)}}+\sum_{m>0,n\le 0}+\sum_{m\le 0,n>0}\right)\frac{1}{E_m-E_n}\langle n|\tau_3|m\rangle\langle m|(1+\gamma^0\gamma^3)\gamma_5\delta_n|n\rangle$$
$$-\langle D_{33}\rangle_{p\uparrow}\cdot\frac{d}{dx}\frac{N_c}{4I}\sum_{\substack{m>0,n>0\\(E_m=E_n)}}\langle n|\tau_3|m\rangle\langle m|(1+\gamma^0\gamma^3)\gamma_5\delta_n|n\rangle. \quad (113)$$

Comparing Eqs. (110) and (113), one notices that the $E_m=E_n$ pieces in the double sums cancels precisely between B' and C terms. (This is true for both of the occupied and nonoccupied expressions.) After some manipulation by taking care of this cancellation, the sum of these two terms can finally be expressed as

$$[\Delta u(x)-\Delta d(x)]^{(1)}_{B'+C}=\langle D_{33}\rangle_{p\uparrow}\cdot M_N\frac{N_c}{2I}\left\{\sum_{\substack{m=all,n\le 0\\(E_m\neq E_n)}}\frac{1}{E_m-E_n}\langle n|\tau_3|m\rangle\langle m|(1+\gamma^0\gamma^3)\gamma_5\delta_n|n\rangle\right.$$
$$-\frac{1}{2M_N}\frac{d}{dx}\sum_{\substack{m=all,n\le 0\\(E_m\neq E_n)}}\langle n|\tau_3|m\rangle\langle m|(1+\gamma^0\gamma^3)\gamma_5\delta_n|n\rangle$$
$$\left.-\sum_{m>0,n\le 0}\frac{1}{E_m-E_n}\langle n|\tau_3|m\rangle\langle m|(1+\gamma^0\gamma^3)\gamma_5\frac{\delta_n+\delta_m}{2}|n\rangle\right\}$$
$$=-\langle D_{33}\rangle_{p\uparrow}\cdot M_N\frac{N_c}{2I}\left\{\sum_{\substack{m=all,n>0\\(E_m\neq E_n)}}\frac{1}{E_m-E_n}\langle n|\tau_3|m\rangle\langle m|(1+\gamma^0\gamma^3)\gamma_5\delta_n|n\rangle\right.$$
$$-\frac{1}{2M_N}\frac{d}{dx}\sum_{\substack{m=all,n>0\\(E_m\neq E_n)}}\langle n|\tau_3|m\rangle\langle m|(1+\gamma^0\gamma^3)\gamma_5\delta_n|n\rangle$$
$$\left.-\sum_{m\le 0,n>0}\frac{1}{E_m-E_n}\langle n|\tau_3|m\rangle\langle m|(1+\gamma^0\gamma^3)\gamma_5\frac{\delta_n+\delta_m}{2}|n\rangle\right\}. \quad (114)$$

For numerical calculation, we shall use the first form for $x>0$, while the second form for $x<0$.

C. $\delta u(x)+\delta d(x)$

Since the evaluation of the transversity distribution can be done in a completely parallel way as the longitudinally polarized distribution functions, we shall show below only the final results. The $O(\Omega^0)$ contribution to $\delta u(x)+\delta d(x)$ vanishes: i.e.,

$$[\delta u(x)+\delta d(x)]^{(0)}=0. \tag{115}$$

The $O(\Omega^1)$ contribution consists of two pieces as

$$[\delta u(x)+\delta d(x)]^{(1)}=[\delta u(x)+\delta d(x)]^{(0)}_{\{A,B\}'}+[\delta u(x)+\delta d(x)]^{(0)}_{C'}, \tag{116}$$

where

$$[\delta u(x)+\delta d(x)]^{(1)}_{\{A,B\}'}=\langle 2J_x\rangle_{pS_x}\cdot M_N\frac{N_c}{2I}\sum_{\substack{m=all,n\leqslant 0\\(E_m\neq E_n)}}\frac{1}{E_m-E_n}\langle n|(\gamma^1\gamma_5-i\gamma^2)\delta_n|m\rangle\langle m|\tau_1|n\rangle$$

$$=-\langle 2J_x\rangle_{pS_x}\cdot M_N\frac{N_c}{2I}\sum_{\substack{m=all,n>0\\(E_m\neq E_n)}}\frac{1}{E_m-E_n}\langle n|(\gamma^1\gamma_5-i\gamma^2)\delta_n|m\rangle\langle m|\tau_1|n\rangle, \tag{117}$$

and

$$[\Delta u(x)+\Delta d(x)]^{(1)}_{C'}=-\langle 2J_x\rangle_{pS_x}\cdot\frac{d}{dx}\frac{N_c}{4I}\sum_{\substack{m=all,n\leqslant 0\\(E_m\neq E_n)}}\langle n|\tau_1|m\rangle\langle m|(\gamma^1\gamma_5-i\gamma^2)\delta_n|n\rangle$$

$$=\langle 2J_x\rangle_{pS_x}\cdot\frac{d}{dx}\frac{N_c}{4I}\sum_{\substack{m=all,n>0\\(E_m\neq E_n)}}\langle n|\tau_1|m\rangle\langle m|(\gamma^1\gamma_5-i\gamma^2)\delta_n|n\rangle. \tag{118}$$

Here $\langle J_x\rangle_{pS_x}$ is defined by

$$\langle J_x\rangle_{pS_x}=\langle pS_x|J_x|pS_x\rangle. \tag{119}$$

D. $\delta u(x)-\delta d(x)$

The $O(\Omega^0)$ contribution is given by

$$[\delta u(x)-\delta d(x)]^{(0)}=\langle D_{31}\rangle_{pS_x}\cdot M_N N_c\sum_{n\leqslant 0}\langle n|\tau_3(\gamma^1\gamma_5-i\gamma^2)\delta_n|n\rangle=-\langle D_{31}\rangle_{pS_x}\cdot M_N N_c\sum_{n>0}\langle n|\tau_3(\gamma^1\gamma_5-i\gamma^2)\delta_n|n\rangle. \tag{120}$$

The $O(\Omega^1)$ contribution consists of two pieces as

$$[\delta u(x)-\delta d(x)]^{(1)}=[\delta u(x)-\delta d(x)]^{(1)}_{[A,B]}+[\delta u(x)-\delta d(x)]^{(1)}_{B'+C} \tag{121}$$

where

$$[\delta u(x)-\delta d(x)]^{(1)}_{[A,B]}=\langle D_{31}\rangle_{pS_x}\cdot M_N\frac{N_c}{8I}i\epsilon_{3cb}\sum_{m>0,n\leqslant 0}\frac{1}{E_m-E_n}$$

$$\times[\langle n|\tau_c|m\rangle\langle m|\tau_b(\gamma^1\gamma_5-i\gamma^2)(\delta_n+\delta_m)|n\rangle+\langle n|\tau_b(\gamma^1\gamma_5-i\gamma^2)(\delta_n+\delta_m)|m\rangle\langle m|\tau_c|n\rangle]$$

$$=-\langle D_{31}\rangle_{pS_x}\cdot M_N\frac{1}{I}\frac{N_c}{2}\sum_{m>0,n\leqslant 0}\frac{1}{E_m-E_n}\Bigg[\langle n|\tau_{+1}|m\rangle\langle n|\tau_{+1}(\gamma^1\gamma_5-i\gamma^2)\frac{\delta_n+\delta_m}{2}|m\rangle$$

$$-\langle n|\tau_{-1}|m\rangle\langle n|\tau_{-1}(\gamma^1\gamma_5-i\gamma^2)\frac{\delta_n+\delta_m}{2}|m\rangle\Bigg], \tag{122}$$

and

$$
\begin{aligned}
[\delta u(x)-\delta d(x)]^{(1)}_{B'+C} &= \langle D_{31}\rangle_{pS_x}\cdot M_N\frac{N_c}{2I}\Bigg\{\sum_{\substack{m=all,n\leqslant 0\\(E_m\neq E_n)}}\frac{1}{E_m-E_n}\langle n|\tau_3|m\rangle\langle m|(\gamma^1\gamma_5-i\gamma^2)\delta_n|n\rangle \\
&\quad -\frac{1}{2M_N}\frac{d}{dx}\sum_{\substack{m=all,n\leqslant 0\\(E_m\neq E_n)}}\langle n|\tau_3|m\rangle\langle m|(\gamma^1\gamma_5-i\gamma^2)\delta_n|n\rangle \\
&\quad -\sum_{m>0,n\leqslant 0}\frac{1}{E_m-E_n}\langle n|\tau_3|m\rangle\langle m|(\gamma^1\gamma_5-i\gamma^2)\frac{\delta_n+\delta_m}{2}|n\rangle\Bigg\}, \\
&= -\langle D_{31}\rangle_{pS_x}\cdot M_N\frac{N_c}{2I}\Bigg\{\sum_{\substack{m=all,n>0\\(E_m\neq E_n)}}\frac{1}{E_m-E_n}\langle n|\tau_3|m\rangle\langle m|(\gamma^1\gamma_5-i\gamma^2)\delta_n|n\rangle, \\
&\quad -\frac{1}{2M_N}\frac{d}{dx}\sum_{\substack{m=all,n>0\\(E_m\neq E_n)}}\langle n|\tau_3|m\rangle\langle m|(\gamma^1\gamma_5-i\gamma^2)\delta_n|n\rangle, \\
&\quad -\sum_{m\leqslant 0,n>0}\frac{1}{E_m-E_n}\langle n|\tau_3|m\rangle\langle m|(\gamma^1\gamma_5-i\gamma^2)\frac{\delta_n+\delta_m}{2}|n\rangle\Bigg\}. \qquad (123)
\end{aligned}
$$

IV. NUMERICAL RESULTS AND DISCUSSION

Before showing the results of numerical calculations, we briefly discuss the parameters of our effective model specified by the Lagrangian (26). Fixing f_π to its physical value, i.e., $f_\pi = 93\,\mathrm{MeV}$, only one parameters of the model is the constituent quark mass M, which plays the role of the coupling constant between the pion and the effective quark fields. There is some argument based on the instanton picture of the QCD vacuum that the value of this mass parameter should not be extremely far from 350 MeV [25]. Phenomenological analyses of various static baryon observables based on this model prefer a slightly larger value of M between 350 MeV and 425 MeV [5,6]. In the present analysis, we use the value $M = 375\,\mathrm{MeV}$ favored from analyses of various static observables of baryons. Actually the model contains ultraviolet divergences so that it must be regularized by introducing some physical cutoff. In the case of static nucleon observables, most frequently used regularization scheme is the one based on Schwinger's proper-time representation [5,6]. Unfortunately, how to generalize this regularization scheme in the evaluation of nucleon structure functions is an open problem. For evaluating quark distribution functions, Diakonov *et al*. then proposed to use the so-called Pauli-Villars regularization scheme, which they claim has several nice properties as compared with the energy cutoff scheme like the proper-time regularization scheme [14]. The basic idea of this regularization scheme is very simple. Using the derivative (gradient) expansion, one can evaluate the effective meson action corresponding to the original effective quark Lagrangian (26) as

$$
\begin{aligned}
S^M_{eff}[U] &= -iN_c\,\mathrm{Sp}\log[i\partial\!\!\!/ - Me^{i\gamma_5\boldsymbol{\tau}\cdot\boldsymbol{\pi}/f_\pi}] \\
&= \frac{4N_c}{f_\pi^2}I_2(M)\cdot\frac{1}{2}(\partial_\mu\boldsymbol{\pi})^2+\cdots. \qquad (124)
\end{aligned}
$$

Here the coefficient of the pion kinetic term given by

$$
I_2(M)\equiv i\int\frac{d^4k}{(2\pi)^4}\frac{M^2}{(k^2-M^2)^2}, \qquad (125)
$$

contains logarithmic divergence. Clearly, this divergence can be removed by introducing a regularized action S^{reg}_{eff} by

$$
S^{reg}_{eff}\equiv S^M_{eff}-\left(\frac{M}{M_{PV}}\right)^2 S^{M_{PV}}_{eff}. \qquad (126)
$$

Here $S^{M_{PV}}_{eff}$ denotes the effective meson action obtained from S^M_{eff} by replacing the dynamical quark mass M with the Pauli-Villars mass M_{PV}. In fact, this replaces $I_2(M)$ with

$$
I_2^{reg}\equiv I_2(M)-\left(\frac{M}{M_{PV}}\right)^2 I_2(M_{PV})=\frac{M^2}{16\pi^2}\log\frac{M^2_{PV}}{M^2}, \qquad (127)
$$

which is clearly finite. Demanding further that the pion kinetic term in S^{reg}_{eff} has the correct normalization, one obtains

$$
\frac{N_c}{4\pi^2}M^2\log\frac{M^2_{PV}}{M^2}=f^2_\pi. \qquad (128)
$$

For $M = 375\,\mathrm{MeV}$, for instance, this gives $M_{PV}\simeq 562\,\mathrm{MeV}$. Other observables like quark distribution functions, which contains logarithmic divergence, can similarly be regularized as

$$
\langle O\rangle^{reg}\equiv\langle O\rangle^M-\left(\frac{M}{M_{PV}}\right)^2\langle O\rangle^{M_{PV}}. \qquad (129)
$$

For the sake of consistency, a soliton solution should also be obtained in the same regularization scheme. The starting-point of soliton construction is the mean field equation

$$
\langle\overline{\psi}\psi\rangle^{reg'}_r\sin F(r)=\langle\overline{\psi}i\gamma_5\boldsymbol{\tau}\cdot\hat{\mathbf{r}}\psi\rangle^{reg'}_r\cos F(r), \qquad (130)
$$

obtained under the assumption of the static hedgehog configuration

$$\hat{\boldsymbol{\pi}}(\boldsymbol{r}) = f_\pi \hat{\boldsymbol{r}} F(r). \tag{131}$$

Here $\langle \bar{\psi}\psi \rangle_r^{reg'}$ and $\langle \bar{\psi} i\gamma_5 \boldsymbol{\tau}\cdot\hat{\boldsymbol{r}}\psi \rangle_r^{reg'}$ are the regularized scalar and pseudoscalar densities in the Pauli-Villars subtraction scheme :

$$\langle \bar{\psi}\psi \rangle_r^{reg'} \equiv \langle \bar{\psi}\psi \rangle_r^{M} - \left(\frac{M}{M_{PV}} \right) \langle \bar{\psi}\psi \rangle_r^{M_{PV}}, \tag{132}$$

$$\langle \bar{\psi}\gamma_5 \boldsymbol{\tau}\cdot\hat{\boldsymbol{r}}\psi \rangle_r^{reg'} \equiv \langle \bar{\psi} i\gamma_5 \boldsymbol{\tau}\cdot\hat{\boldsymbol{r}}\psi \rangle_r^{M} - \left(\frac{M}{M_{PV}} \right) \times \langle \bar{\psi} i\gamma_5 \boldsymbol{\tau}\cdot\hat{\boldsymbol{r}}\psi \rangle_r^{M_{PV}}. \tag{133}$$

Recently, self-consistent solutions of this equation of motion has been obtained in [26] with use of the Kahana-Ripka basis [27]. (Essentially the same equation was solved in [28] within the framework of the Nambu–Jona Lasinio model with an *ad hoc* nonlinear constraint.) However, one should use this regularization scheme with some care. In fact, it is known that the single subtraction is not enough to get rid of linear divergences, for instance, contained in the expression of the vacuum quark condensate [28], which implies that $\langle \bar{\psi}\psi \rangle_r^{reg'}$ and $\langle \bar{\psi} i\gamma_5 \boldsymbol{\tau}\cdot\hat{\boldsymbol{r}}\psi \rangle_r^{reg'}$ also contain convergences. Why could the authors of Refs. [26,28] obtain self-consistent solutions then? The reason is in the way of solving the equation of motion (129) in the nonlinear model. Given an appropriate initial form of $F(r)$, one can evaluate $\langle \bar{\psi}\psi \rangle_r^{reg'}$ and $\langle \bar{\psi} i\gamma_5 \boldsymbol{\tau}\cdot\hat{\boldsymbol{r}}\psi \rangle_r^{reg'}$ by using the Kahana-Ripka plane-wave basis as long as the box size D and the maximum momentum k_{max} are finite. A new $F(r)$ can then be obtained from

$$F(r) = \arctan\left(\frac{\langle \bar{\psi} i\gamma_5 \boldsymbol{\tau}\cdot\hat{\boldsymbol{r}}\psi \rangle_r^{reg'}}{\langle \bar{\psi}\psi \rangle_r^{reg'}} \right). \tag{134}$$

As k_{max} increases, both of $\langle \bar{\psi}\psi \rangle_r^{reg'}$ and $\langle \bar{\psi} i\gamma_5 \boldsymbol{\tau}\cdot\hat{\boldsymbol{r}}\psi \rangle_r^{reg'}$ tend to diverge. We numerically find that both quantifies increases at the same rate as k_{max} increases so that the resultant $F(r)$ is quite insensitive to the value of k_{max} for large enough k_{max}. This is the reason why stable soliton solutions could be found in the above mentioned single-subtraction Pauli-Villars regularization scheme. The existence of finite energy soliton could also be inferred from the derivative expansion analysis of the nonlinear Lagrangian (124) with vanishing current quark masses. Nevertheless, one should keep in mind that it is not a completely satisfactory scheme in the sense that its predictions for some special quantities like the vacuum quark condensate contain divergences. For obtaining satisfactory answers also for these special quantities, the single-substraction Pauli-Villars scheme is not enough. We found that more sophisticated Pauli-Villars scheme with two substraction meets this requirement, and that its self-consistent solutions are only slightly different from those of the naive single-subtraction scheme, except when discussing some special quantities as pointed out above. (This analysis will be reported elsewhere.) Considering the fact that the calculation of the structure functions are very time-consuming, we shall then use here the single-subtraction Pauli-Villars scheme, keeping in mind that some particular observables are out of the application of this regularization scheme. Finally, as for the nucleon mass, we prefer to using the theoretical soliton mass $M_N \simeq 1102\,\mathrm{MeV}$ rather than the physical mass, since it respects the energy-momentum sum rule at the energy scale of the model.

For evaluating quark distribution functions at the $O(\Omega^1)$, we must perform infinite double sums over all the single-quark orbitals which are eigenstates of the static Hamiltonian H given by Eq. (31). As far as static nucleon observables, a numerical technique for carrying out such double sums was established in [5]. On the other hand, several new subtleties arising in the evaluation of quark distribution functions have been explained in [17]. In the actual numerical calculation, the expression of each physical quantity is divided into two pieces, i.e., the contribution of what we call the valence quark level (it is the lowest energy eigenstate of the static Dirac Hamiltonian H, which emerges from the positive energy continuum) and that of the Dirac sea quarks (or the vacuum polarization contribution) as explained in [17]. The regularization is introduced into the latter part only.

As was stated in the paragraph below Eq. (89), our numerical analysis relies crucially upon the assumed equivalence of distribution functions given as sums over the occupied and nonoccupied quark orbitals. In view of its important role played in our whole analysis, it is desirable if we can verify this equivalence also numerically. The identity which we want to show numerically is Eq. (90), or equivalently

$$A(x) + B(x) = 0, \tag{135}$$

with

$$A(x) = M_N \frac{1}{I} \frac{N_c}{2} \sum_{\substack{m=all, n=all \\ (E_m \neq E_n)}} \frac{1}{E_m - E_n} \times \langle n|\tau_3|m\rangle \langle m|(1+\gamma^0\gamma^3)\gamma_5 \delta_n|n\rangle, \tag{136}$$

$$B(x) = \frac{d}{dx} \frac{1}{2I} \frac{N_c}{2} \times \sum_{\substack{m=all, n=all \\ (E_m = E_n)}} \langle n|\tau_3|m\rangle \langle m|(1+\gamma^0\gamma^3)\gamma_5 \delta_n|n\rangle. \tag{137}$$

Using the well-established identity [13,14]

$$0=\sum_{n=all}\langle n|\tau_3(1+\gamma^0\gamma^3)\gamma_5\delta_n|n\rangle$$

$$=\sum_{\substack{m=all,n=all\\(E_m\neq E_n)}}\langle n|\tau_3|m\rangle\langle m|(1+\gamma^0\gamma^3)\gamma_5\delta_n|n\rangle$$

$$+\sum_{\substack{m=all,n=all\\(E_m=E_n)}}\langle n|\tau_3|m\rangle\langle m|(1+\gamma^0\gamma^3)\gamma_5\delta_n|n\rangle, \tag{138}$$

$B(x)$ can also be expressed as

$$B(x)=-\frac{d}{dx}\frac{1}{2I}\frac{N_c}{2}\sum_{\substack{m=all,n=all\\(E_m\neq E_n)}}\langle n|\tau_3|m\rangle$$

$$\times\langle m|(1+\gamma^0\gamma^3)\gamma_5\delta_n|n\rangle. \tag{139}$$

In the actual numerical calculation of $B(x)$, we use this latter form given as a derivative of a double sum over the single-quark orbitals, since the effect of working in a finite model space (i.e., with finite values of k_{max} and D) can be reduced by using this latter expression rather than Eq. (137). The numerical derivative here is performed after calculating the double sum by using the method explained in [17]. The solid and dash-dotted curves in Fig. 1(a) respectively stand for the numerical results for $A(x)$ and $B(x)$, while their sum is shown by the dotted curve. [This sum is shown also in Fig. 1(b) with a different scale.] One sees that the two terms $A(x)$ and $B(x)$ are nearly cancelled. Unfortunately, each of $A(x)$ and $B(x)$ has quite a large absolute value and their sum turns out to have a fluctuating behavior around zero with the amplitude of the order of quark distributions which we want to obtain. The fluctuation is especially violent near $x\simeq 0$. Undoubtedly, the best we can say on the basis of the present numerical analysis is that the sum of $A(x)$ and $B(x)$ is *not inconsistent* with zero. However, we find that such a fluctuating behavior with large amplitude also appears when we evaluate the corresponding distribution function using the theoretical formula given as a occupied sum for $x<0$ and a nonoccupied sum for $x>0$. This is due to a delicate cancellation of two large numbers, i.e., the main contribution and the corresponding vacuum subtraction term (obtained with $U=1$). This should be contrasted to the case of using the theoretical expression given as an occupied sum for $x>0$ and a nonoccupied sum for $x<0$. (Note that one can always rewrite the formulas for the distribution functions in either of the occupied or nonoccupied form, once the above identity is assumed.) In this case, the vacuum subtraction term identically vanishes and there is no necessity of handling delicate cancellation of large numbers. This is the reason why we always want to rewrite the formulas for distribution functions in either of the occupied form or the nonoccupied form according to the sign of x by assuming the above identity. We illustrate in Fig. 2 the merit of evaluating distribution functions in this way. The solid and dotted curves in Fig. 2(a) respectively stand for the bare results for the valence and vacuum polarization contributions to the $[\Delta u(x)+\Delta d(x)]^{(1)}_{\{A,B\}}$, term in Eq. (97), obtained with use of the discretized momentum basis of Kahana and Ripka, while the two curves in Fig. 2(b) represent the corresponding contributions to the $[\Delta u(x)+\Delta d(x)]^{(1)}_{C'}$ term before the numerical derivative over x. (We recall that the discontinuous behavior of the shown distribution functions comes from the use of the discretized Kahana-Ripka basis. The physical distribution functions, which are continuous functions of x, can be obtained by using either of the smearing method advocated in [13,14] or the least-square-fitting procedure used in [17]. The numerical derivative over x in $[\Delta u(x)+\Delta d(x)]^{(1)}_{C'}$ term becomes practicable only after this procedure.) We first notice that there is no significant fluctuation in the vacuum polarization contribution to the $[\Delta u(x)+\Delta d(x)]^{(1)}_{C'}$ term. Furthermore, even the fluctuation of the vacuum polarization contribution to $[\Delta u(x)+\Delta d(x)]^{(1)}_{\{A,B\}}$, is seen to have much smaller amplitude as compared with the one observed in Fig. 1(b). It is in fact much smaller than unity, the typical scale of the relevant distribution function, provided by the contribution of the discrete level. We therefore expect that, although the important identity (135) cannot be proved with the same numerical accuracy, the total distribution function themselves can be evaluated with some reliable accuracy, once Eq. (135) is assumed.

Summarizing the above argument, although our numerical proof shown in Fig. 1 is far from complete, the observed cancellation of the two terms, which have nontrivial x dependences, cannot be accidental. We also recall that the equivalence of the occupied and nonoccupied expressions follows basically from the anticommutation relation of the quark fields at spacelike separation and this anticommutation relation is not affected by the regularization with use of the Pauli-Villars subtraction [13,14,20]. We therefore assume it throughout the following numerical analysis with the hope that more complete numerical proof will be provided by near future investigations.

Now we start to show the results of our numerical calculation for polarized quark distribution functions of the nucleon. Shown in Fig. 3 are the $O(\Omega^0)$ contributions to the isovector longitudinally polarization distribution functions $\Delta u(x)-\Delta d(x)$ (solid curves) and $\Delta\overline{u}(x)-\Delta\overline{d}(x)$ (dashed curves), which was first calculated by Diakonov *et al.* [14]. Here Fig. 3(a) represents the contributions of the discrete valence quark level, while Fig. 3(b) is the vacuum polarization contribution to the same quantities. Sum of these two contributions are shown in Fig. 3(c). As shown by Diakonov *et al.*, the $O(\Omega^0)$ vacuum polarization contributions to $\Delta u(x)-\Delta d(x)$ and $\Delta\overline{u}(x)-\Delta\overline{d}(x)$ are fairly large. [The large and positive longitudinal polarization of the isovector combination of the antiquark distributions seems to be a characteristic prediction of the CQSM, which can in principle be tested by the improved phenomenological analyses of polarized parton distribution functions in the near future. More detailed discussion on this point will be given after finishing the evaluation of the $O(\Omega^1)$ contribution to the

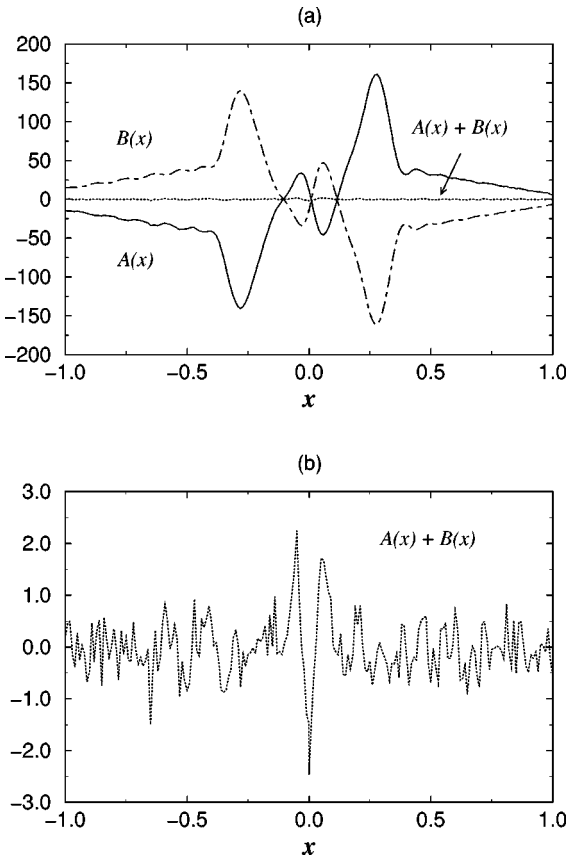

FIG. 1. Numerical check of the identity (135) on which the equivalence of the occupied and nonoccupied expressions for the polarized quark distribution functions is based. The solid and dash-dotted curves in (a) respectively stand for the numerical results for $A(x)$ and $B(x)$ in Eq. (135), while their sum is shown by the dotted curve in (a) and also in (b) with a different scale.

same distribution function as well as that of the isoscalar longitudinally polarized distribution functions.]

Next, we show in Fig. 4 the $O(\Omega^1)$ contribution to the same distribution functions $\Delta u(x)-\Delta d(x)$ and $\Delta\bar{u}(x)-\Delta\bar{d}(x)$. Figures 4(a), 4(b) and 4(c) respectively stand for the $O(\Omega^1)$ contributions of the discrete valence quark level, those of the Dirac sea quarks (or the vacuum polarization contributions), and their sums. One sees that the $O(\Omega^1)$ contributions to the isovector longitudinally polarized distribution function are far from negligible as compared with the leading $O(\Omega^0)$ contributions. This could be expected since the first moment of this distribution functions gives the isovector axial coupling constant of the nucleon

$$g_A^{(3)}=\int_0^1\{[\Delta u(x)-\Delta d(x)]+[\Delta\bar{u}(x)-\Delta\bar{d}(x)]\}dx, \tag{140}$$

while we already know from the previous analyses that the $O(\Omega^1)$ contribution to $g_A^{(3)}$ is large enough to resolve the longstanding g_A problem in the hedgehog soliton model [29,30,24]. Adding this $O(\Omega^1)$ contribution to the leading $O(\Omega^0)$ contribution, we obtain final answers for $\Delta u(x)-\Delta d(x)$ and $\Delta\bar{u}(x)-\Delta\bar{d}(x)$, which will be shown later together with the final answer for the isoscalar longitudinal distribution functions $\Delta u(x)+\Delta d(x)$ and $\Delta\bar{u}(x)+\Delta\bar{d}(x)$. Before showing those, we give in Fig. 5 the result for the $O(\Omega^1)$ contributions to the isoscalar longitudinally polarized distribution functions, $\Delta u(x)+\Delta d(x)$ and $\Delta\bar{u}(x)+\Delta\bar{d}(x)$. [We recall that there is no $O(\Omega^0)$ contribution to these distribution functions.] Figures 5(a), 5(b) and 5(c) respectively stand for the contributions of the discrete valence quark level, those of the vacuum polarization contributions, and their sums. One sees that the vacuum polarization contributions to the distribution functions $\Delta u(x)+\Delta d(x)$ and $\Delta\bar{u}(x)+\Delta\bar{d}(x)$ are much smaller than those of the corresponding isovector distributions $\Delta u(x)-\Delta d(x)$ and $\Delta\bar{u}(x)-\Delta\bar{d}(x)$. Now we show in Fig. 6 the final answers for $\Delta u(x)-\Delta d(x)$ and $\Delta\bar{u}(x)-\Delta\bar{d}(x)$, which are the sums of the $O(\Omega^0)$ and $O(\Omega^1)$ contributions, in comparison with the final answers for $\Delta u(x)+\Delta d(x)$ and $\Delta\bar{u}(x)+\Delta\bar{d}(x)$ arising from the $O(\Omega^1)$ terms alone. We observe quite a big difference between the isovector distributions and the isoscalar one. The overall magnitude of $\Delta u(x)+\Delta d(x)$ is much smaller than that of $\Delta u(x)-\Delta d(x)$, which denotes that u-quark is positively polarized, while the d-quark is negatively polarized to the direction of proton spin.

At this stage, it may be interesting to compare our theoretical predictions for the longitudinally polarized quark distribution functions with some of the semiphenomenological parametrization. The parametrization given by Glück, Reya, Stratmann, and Vogelsang (GRSV) is especially convenient for the purpose of handy comparison [31], since the normalization point ($Q^2_{init}\simeq 0.34\,\mathrm{GeV}^2$) of their parametrization is fairly close to the energy scale of our effective quark model ($M^2_{PV}\simeq 0.32\,\mathrm{GeV}^2$). Figure 7 shows this comparison. The filled squares in Fig. 7(a) and Fig. 7(b) stand for the GRSV parametrizations for the quark distribution functions $x(\Delta u(x)+\Delta\bar{u}(x)+\Delta d(x)+\Delta\bar{d}(x))$ and $x(\Delta u(x)+\Delta\bar{u}(x)-\Delta d(x)-\Delta\bar{d}(x))$, respectively. Of the two theoretical curves in each figure, the solid curve is the answer of the present calculation, whereas the dashed curve is obtained by using the old treatment used in [17], which amounts to dropping some of the nonlocality effects in time. One observes that the nonlocality corrections newly introduced in the present analysis are quite important especially for the isoscalar distribution $x(\Delta u(x)+\Delta\bar{u}(x)+\Delta d(x)+\Delta\bar{d}(x))$, while it is less important for the isovector distribution $x(\Delta u(x)+\Delta\bar{u}(x)-\Delta d(x)-\Delta\bar{d}(x))$. [This is probably because the nonlocality corrections appearing at the $O(\Omega^1)$ are masked by the dominant $O(\Omega^0)$ contribution in the case of isovector polarized distribution functions.] By comparing the two theoretical curves for $x(\Delta u(x)+\Delta\bar{u}(x)+\Delta d(x)+\Delta\bar{d}(x))$ with the corresponding GRSV parametrization, one finds that the new treatment leads to a better agreement. Especially impressive is that the new treatment reproduces the negative sign of the GRSV distribution function in the smaller x region, although one should not forget the fact that the GRSV parametrizations are not experimental data themselves. We

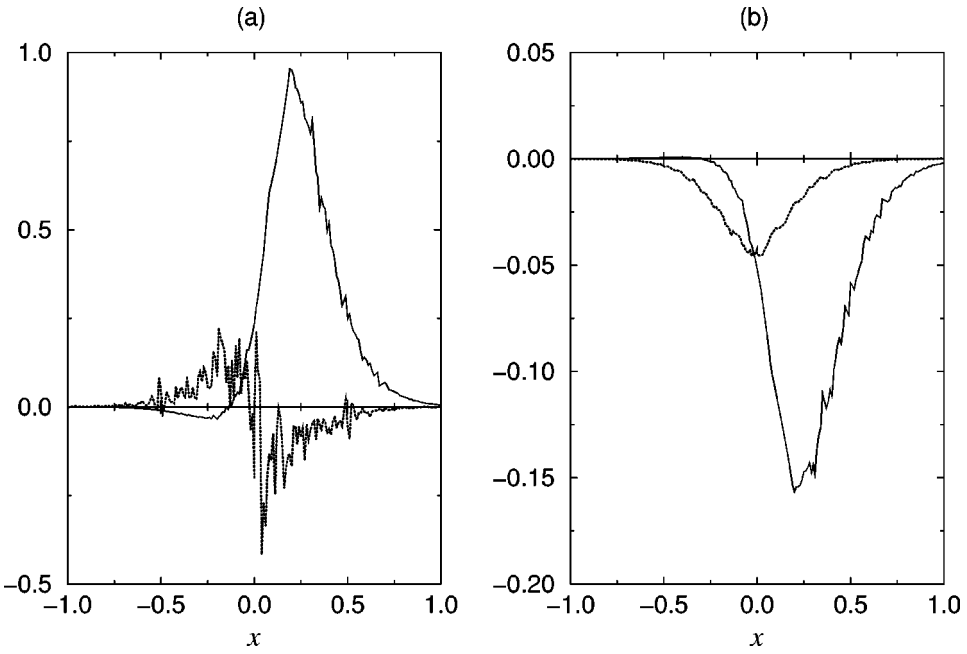

FIG. 2. The solid and dotted curves in (a) respectively stand for the bare results for the valence and vacuum polarization contributions to the $[\Delta u(x)+\Delta d(x)]^{(1)}_{\{A,B\}'}$ term in Eq. (97), obtained with use of the discretized momentum basis of Kahana and Ripka, while the two curves in (b) represent the corresponding contributions to the $[\Delta u(x)+\Delta d(x)]^{(1)}_{C'}$ term before the numerical derivative over x. The vacuum polarization contributions have been evaluated by using the occupied expression for $x>0$ and the nonoccupied one for $x<0$.

point out that the most important factor leading to this qualitative difference between the old and new treatments of the quark distribution functions is the nonlocality correction arising from the second term of Eq. (38), i.e., the proper account of nonlocality in time of the operator $A^{\dagger}(0)O_a A(z_0)$.

Turning back to Fig. 6, let us inspect the theoretical predictions for the antiquark distributions in more detail. An interesting feature is that, in most region of x, $\Delta\bar{u}(x)-\Delta\bar{d}(x)>0$ and $\Delta\bar{u}(x)+\Delta\bar{d}(x)<0$ with the relation $|\Delta\bar{u}(x)-\Delta\bar{d}(x)|\gg|\Delta\bar{u}(x)+\Delta\bar{d}(x)|$. This denotes that $\bar{d}$ is strongly polarized in the opposite direction to the proton spin, while $\bar{u}$ is weakly polarized in the same direction to the proton spin. This appears to be a prominent prediction of the CQSM, which is worthy of special mention. In fact, it sharply contradicts the assumption of SU(2) symmetric sea quark polarization $\Delta\bar{u}(x)=\Delta\bar{d}(x)$, which is frequently used in semiphenomenological analyses of parton distributions. The isospin symmetric polarization is also assumed in the analysis by Glück, Reya, Stratmann and Vogt [31]. We compare in Fig. 8 our prediction for the $x\Delta\bar{u}(x)$ and $x\Delta\bar{d}(x)$ with the GRSV parametrization, which assumes that $x\Delta\bar{u}(x)=x\Delta\bar{d}(x)[\equiv x\Delta\bar{q}(x)]$. Naturally, one finds qualitative difference between the theoretical distributions and the GRSV parametrization. Still, it is interesting to see that the average of the two theoretical distributions $x\Delta\bar{u}(x)$ and $x\Delta\bar{d}(x)$ is not extremely different from the corresponding GRSV parametrization $x\Delta\bar{q}(x)$. As for the unpolarized distribution functions, the breakdown of the assumption of SU(2) symmetric sea has already been confirmed by the New Muon Collaboration (NMC) measurement [16]. By the same token, there is no compelling reason to believe that the spin dependent antiquark (sea quark) distributions are isospin symmetric. In fact, our previous analyses based on the same model shows that the isospin asymmetry of the unpolarized

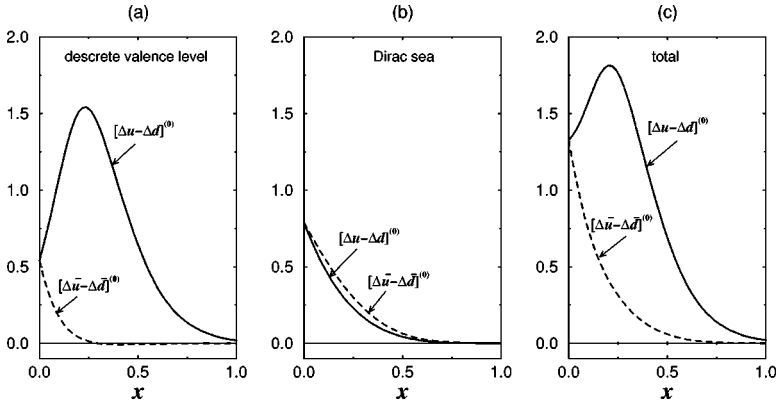

FIG. 3. The $O(\Omega^0)$ contributions to the isovector longitudinally polarized distribution functions $\Delta u(x)-\Delta d(x)$ (solid curves) and $\Delta\bar{u}(x)-\Delta\bar{d}(x)$ (dashed curves). Here the three figures (a), (b), and (c) correspond to the contributions of the discrete valence level, those of the Dirac sea quarks, and their sums, respectively.

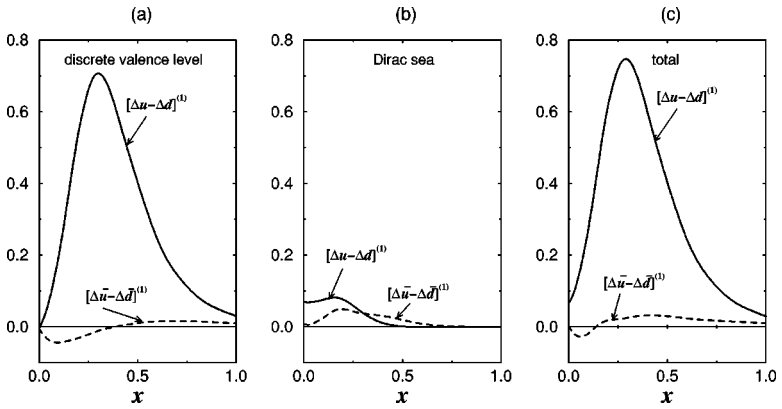

FIG. 4. The $O(\Omega^1)$ contributions to the isovector longitudinally polarized distribution functions $\Delta u(x)-\Delta d(x)$ (solid curves) and $\Delta\bar{u}(x)-\Delta\bar{d}(x)$ (dashed curves). The meaning of the three figures (a), (b), and (c) is the same as in Fig. 2.

sea quark distributions can be explained very naturally as combined effects of two ingredients, i.e., the apparently existing flavor asymmetry of valence quark numbers in the nucleon and the spontaneous chiral symmetry breaking of QCD vacuum [17–19]. It is just the same mechanism that is responsible for the opposite longitudinal polarization of the $\bar{u}$ and $\bar{d}$ quarks.

The above-mentioned fairly big difference between the isovector and isoscalar longitudinally polarized distribution functions manifests itself also in their first moments, i.e., the isovector and isoscalar axial charges given as

$$g_A^{(3)}=\int_0^1\{[\Delta u(x)-\Delta d(x)]+[\Delta\bar{u}(x)-\Delta\bar{d}(x)]\}dx\simeq 1.41, \tag{141}$$

$$g_A^{(0)}=\int_0^1\{[\Delta u(x)+\Delta d(x)]+[\Delta\bar{u}(x)+\Delta\bar{d}(x)]\}dx\simeq 0.35. \tag{142}$$

The resultant large isovector axial charge and small isoscalar (flaver-singlet) one seem to be qualitatively consistent with the observation. Especially interesting here is the flavor-singlet axial charge identified with the quark spin content of the nucleon. In the context of the CQSM, this quantity was first investigated in [5] with use of the self-consistent soliton solution obtained in the proper-time regularization scheme. The value of $g_A^{(0)}=\langle\Sigma_3\rangle$ obtained there ranges from 0.4 to 0.5 corresponding to the variation of the dynamical quark mass M from 425 MeV to 375 MeV. One may notice that the value $g_A^{(0)}\simeq 0.35$ obtained in the present calculation is a little smaller than the previous one. The cause of this difference can be traced back to the qualitative change of the self-consistent soliton solution obtained in the new regularization scheme. As a general trend, the Pauli-Villars regularization scheme cuts off high momentum components more weakly than the energy-cutoff scheme like the proper-time one, thereby leading to soliton solutions with stronger distortion. Incidentally, owing to the nucleon spin sum rule $\langle L_3\rangle+\frac{1}{2}\langle\Sigma_3\rangle=\frac{1}{2}$ proved in [5], the rest of the nucleon spin is carried by the orbital angular momentum of the effective quark fields. (Naturally, this is true only at low Q^2 corresponding to the energy scale of our effective model. It will be shown later that an increasing portion of the nucleon spin is carried by gluons as Q^2 increases.) A soliton with stronger distortion gives larger orbital angular momentum, and consequently smaller quark spin fraction [5].

The characteristic feature of the above theoretical prediction, i.e., larger isovector charge and smaller isoscalar one seems also consistent with the idea of N_c counting or $1/N_c$ expansion of QCD. For understanding it, we just recall the fact that the collective angular velocity Ω scales as $1/N_c$, so that the leading contributions to the isovector and isoscalar polarized distribution functions are respectively of the $O(N_c^1)$ and $O(N_c^0)$. The detailed comparison of the theoretical first moments with the corresponding experimental data will be given later after taking account of the scale dependence of them.

Now we show the results of our numerical calculation for transversity distributions. Figure 9 shows the $O(\Omega^0)$ contri-

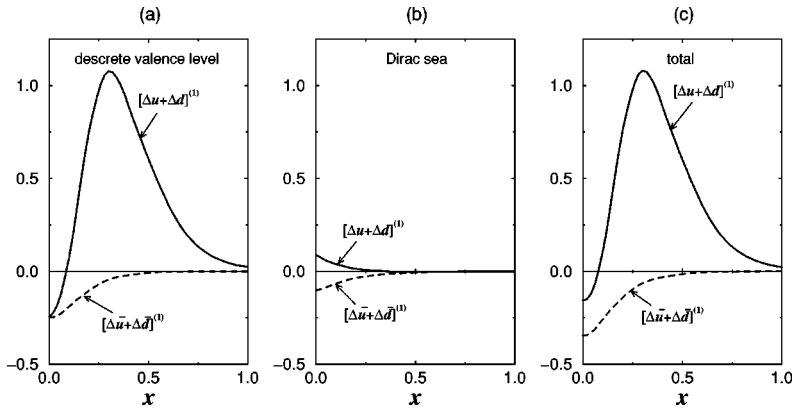

FIG. 5. The $O(\Omega^1)$ contributions to the isoscalar longitudinally polarized distribution functions $\Delta u(x)+\Delta d(x)$ (solid curves) and $\Delta\bar{u}(x)+\Delta\bar{d}(x)$ (dashed curves). The meaning of the three figures (a), (b), and (c) is the same as in Fig. 2.

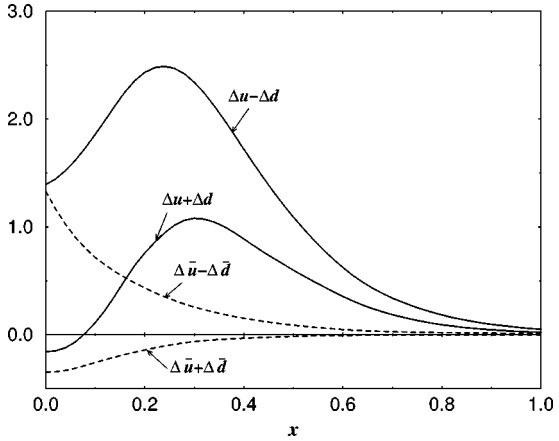

FIG. 6. The final predictions of the CQSM for the longitudinally polarized distribution functions $\Delta u(x)-\Delta d(x)$ and $\Delta\overline{u}(x)-\Delta\overline{d}(x)$ given as the sums of the $O(\Omega^0)$ and $O(\Omega^1)$ contributions, in comparison with those for the isoscalar longitudinally polarized distribution functions $\Delta u(x)+\Delta d(x)$ and $\Delta\overline{u}(x)+\Delta\overline{d}(x)$ coming from the $O(\Omega^1)$ terms.

butions to the isovector transversity distribution functions $\delta u(x)-\delta d(x)$ (solid curves) and $\delta\overline{u}(x)-\delta\overline{d}(x)$ (dashed curves). Here Fig. 9(a) stand for the contributions of the discrete valence level, while Fig. 9(b) represent the vacuum polarization contributions to the same quantities. The sums of these two contributions are shown in Fig. 9(c). One finds that the vacuum polarization contributions to these distribution functions are fairly small. Incidentally, within the context of the CQSM, the isovector transversity distribution function was investigated by Pobylitsa and Polyakov for the first time [32]. Our answer shown in Fig. 9(a) is qualitatively consistent with their result which takes account of the contribution of the discrete valence level only. They also gave some argument in favor of the suppression of the Dirac continuum contribution to $\delta u(x)-\delta d(x)$ by using the knowledge of the derivative expansion together with the first moment sum rule. Now it appears that their conjecture gains quantitative support by our explicit calculation of the Dirac sea contribution. Note, however, that their calculation for $\delta u(x)-\delta d(x)$ cannot be taken as a final one, which can be compared with some phenomenological distribution. This is because it has not yet included potentially important $O(\Omega^1)$ contributions discussed below. Now, we show in Fig. 10 our result for the $O(\Omega^1)$ contributions to the same transversity distribution functions $\delta u(x)-\delta d(x)$ and $\delta\overline{u}(x)-\delta\overline{d}(x)$. Also for these $O(\Omega^1)$ terms, the vacuum polarization contributions turn out to be very small as compared with the contributions of the discrete valence quark level. However, one should note that the valence level contribution at the $O(\Omega^1)$ is far from small as compared with the leading $O(\Omega^0)$ contributions, and should not be discarded. Next we show in Fig. 11 the theoretical isoscalar transversity distributions resulting at the $O(\Omega^1)$. One sees that vacuum polarization contribution is quite small again. The final predictions of the CQSM for $\delta u(x)-\delta d(x)$ and $\delta\overline{u}(x)-\delta\overline{d}(x)$, which are the sums of the $O(\Omega^0)$ and $O(\Omega^1)$ contributions, are shown in Fig. 12, in comparison with the final answers for $\delta u(x)+\delta d(x)$ and $\delta\overline{u}(x)+\delta\overline{d}(x)$ arising from the $O(\Omega^1)$ terms. One again sees that the magnitudes of the isoscalar distributions are much smaller than those of the isovector distributions in consistency with the N_c counting rule. Remember the similar observation made before for the longitudinally polarized distribution functions. To see it in more detail, we find that the ratio of the isoscalar to isovector distribution is much smaller for the longitudinally polarized distribution than for the transversity one. We shall come back later to this point when discussing the corresponding first moments of these spin dependent quark distribution functions.

The transversity distribution functions have also been investigated by Gamberg *et al.* [12] based on the Nambu–Jona–Lasinio soliton model with an *ad hoc* nonlinear constraint, which is essentially equivalent to the CQSM. In view of the above observation that the Dirac sea contributions play no significant role at least for the transversity distributions, it appears that their calculation carried out under the ''valence

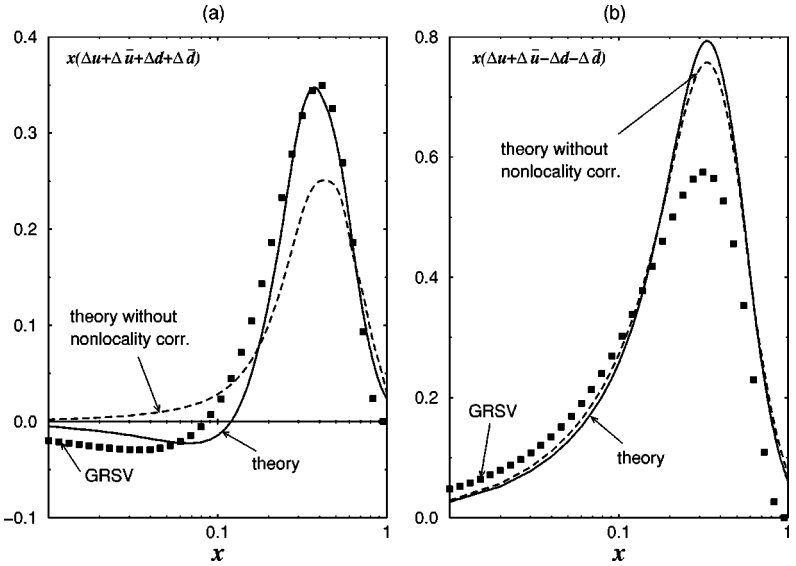

FIG. 7. The theoretical predictions for the longitudinally polarized distribution functions, $x(\Delta u(x)+\Delta\overline{u}(x)+\Delta d(x)+\Delta\overline{d}(x))$ and $x(\Delta u(x)+\Delta\overline{u}(x)-\Delta d(x)-\Delta\overline{d}(x))$, are compared with the corresponding semi-phenomenological parametrization given by Glück, Reya, Stratmann and Vogelsang [31]. Of the two theoretical curves in each figure, the solid curve is the answer of the present calculation, whereas the dashed curve is obtained by using the old treatment used in [17], which amounts to dropping some of the nonlocality effects in time.

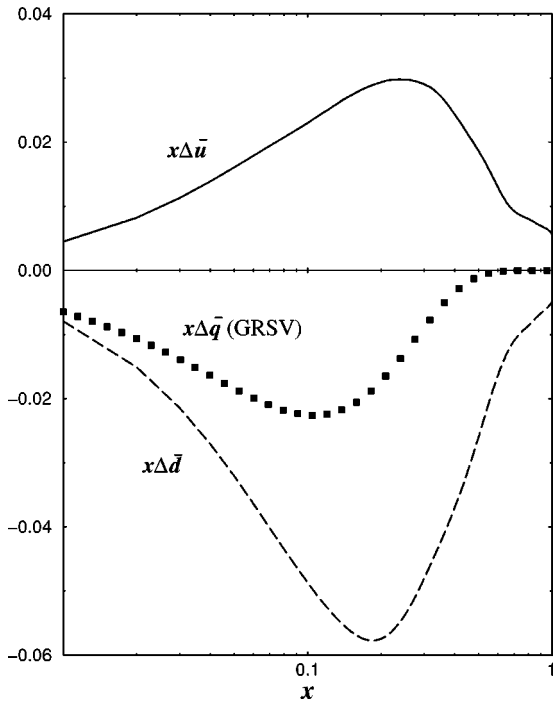

FIG. 8. The predictions of the CQSM for the polarized antiquark distributions $x\Delta\overline{u}(x)$ and $x\Delta\overline{d}(x)$ are compared with the corresponding GRSV parametrization, which assumes SU(2) symmetric sea quark polarization, $x\Delta\overline{u}(x)=x\Delta\overline{d}(x)[\equiv x\Delta\overline{q}(x)]$.

quark approximation'' might be justified and that their results should essentially coincide with ours. However, several important differences between their analysis and ours should not be overlooked. The first concerns the nonlocality correction in time, which was properly taken into account in our present analysis but was totally neglected in their treatment. Note that the most important piece of it is included in Eq. (118) for $\delta u(x)+\delta d(x)$ and in Eq. (123) for $\delta u(x)-\delta d(x)$. As was already shown in the case of the isoscalar longitudinally polarized distribution $\Delta u(x)+\Delta d(x)$, this nonlocality correction in time plays quite an important role even under the ''valence quark approximation.'' Secondly, in the calculation of the isovector transversity distribution function, they have included only the $O(\Omega^0)$ contribution and dropped the $O(\Omega^1)$ term intentionally. The reason is based on their claim that this $O(\Omega^1)$ contribution arises only when one adopts a particular ordering of the operators in the collective space and that in the case of the isovector axial charge, $g_A^{(3)}$, the introduction of the corresponding term leads to a significant violation of PCAC (partial conservation of axial vector current) relation. That this claim is not justified was already discussed in [24] to the full extent, so that we do not repeat it here. We just want to mention that the introduction of this $O(\Omega^1)$ correction also seems to be required by phenomenology. In fact, as admitted by themselves, dropping of this contribution leads to sizable underestimation of the isovector axial charge $g_A^{(3)}$. This in turn indicates that it would also lead to a considerable underestimation of the isovector tensor charge. To sum up, by comparing the numerical results of our analysis and theirs, they naturally share many qualitative features in common. To see it in more detail, however, there appear to be some quantitative differences especially for the transversity distribution for d-quark. The above-mentioned differences of the two theoretical analyses, i.e., the $O(\Omega^1)$ contribution to the isovector transversity distribution and the nonlocality correction in time to the isoscalar one are likely to be the main cause of these quantitative discrepancies.

Roughly speaking, the quark distribution functions evaluated here corresponds to the energy scale of the order of the Pauli-Villars cutoff mass $M_{PV}\simeq 0.56\,\mathrm{GeV}$. The Q^2 evolution must be taken into account in some way before comparing them with the observed nucleon structure functions at high Q^2. Recently, Saga group provided a Fortran program, which gives numerical solution of Dokshitzer-Gribov-Altarelli-Parisi (DGLAP) evolution equations at the next-to-leading order (NLO) for the polarized as well as unpolarized structure functions of the nucleon [33–35]. We shall make use of their Fortran programs to evaluate the polarized distribution functions at large Q^2 [34,35]. The question here is what value we should take for the initial energy scale of this Q^2 evolution. Since the use of perturbative QCD below 1 GeV is anyhow questionable, one may take this initial energy scale Q^2_{init} as an adjustable parameter, which would be fixed by adjusting the observed structure functions at high energy region. Here we have tried to see the effect of variation of Q^2_{init} in a small range of Q^2 around the model energy scale of $M^2_{PV}\simeq(0.56\,\mathrm{GeV})^2$. The value $Q^2_{init}=(0.5\,\mathrm{GeV})^2=0.25\,\mathrm{GeV}^2$ obtained from this analysis will be used throughout the following investigation. Before showing the

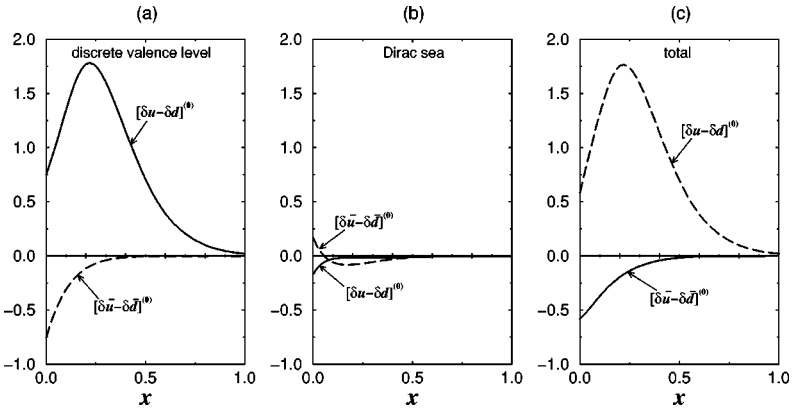

FIG. 9. The $O(\Omega^0)$ contributions to the isovector transversity distribution functions $\delta u(x)-\delta d(x)$ (solid curves) and $\delta\overline{u}(x)-\delta\overline{d}(x)$ (dashed curves). Here the three figures (a), (b), and (c) correspond to the contributions of the discrete valence level, those of the Dirac sea quarks, and their sums, respectively.

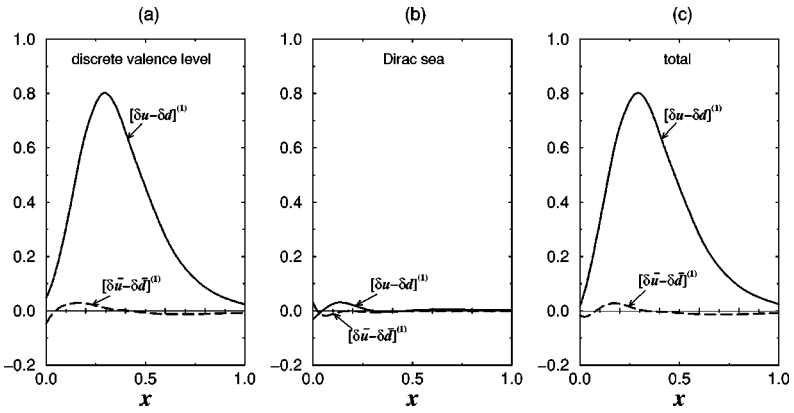

FIG. 10. The $O(\Omega^1)$ contributions to the isovector transversity distribution functions $\delta u(x) - \delta d(x)$ (solid curves) and $\delta\overline{u}(x) - \delta\overline{d}(x)$ (dashed curves). The meaning of the three figures (a), (b), and (c) is the same as in Fig. 2.

results of Q^2 evolution, we want to make a short comment. One notices from the figures given so far, the distribution functions evaluated in our effective model have unphysical tails beyond $x>1$, although they are not so significant. These unphysical tails of the theoretical distribution functions come from an approximate nature of our treatment of the soliton center-of-motion (as well as the collective rotational motion), which is essentially nonrelativistic. A simple procedure to remedy this defect was proposed by Jaffe based on the $(1+1)$ dimensional bag model [36] and recently reinvestigated by Gamberg *et al.* within the context of the NJL soliton model [37]. According to the latter authors [37], the effect of Lorentz contraction can effectively be taken into account by first evaluating the distribution functions in the soliton rest frame (as we are doing here) and then by using a simple analytical transformation that preserves first moments of distribution functions, as far as the $O(\Omega^0)$ contributions to the distribution functions are concerned. Such a simple relation may not be expected however if we consider the rotational motion of the soliton, which are anyhow three dimensional. In fact, a comparison with the corresponding phenomenological distribution functions seems to indicate that the above procedure based on the $(1+1)$ dimensional dynamics tends to overestimate the effect of Lorentz contraction. In the present investigation, we therefore decided not to use their procedure. Still we want distribution functions which vanish outside the range $0<x<1$ so that we can use the Q^2-evolution Fortran program provided by Saga group [34,35]. Since the unphysical tails of our theoretical distributions are rather small in magnitude, we are to use a simple cutoff procedure as follows. That is, we obtain modified distribution functions, which can be used as input distributions of the above Fortran program, from the original theoretical distribution functions by multiplying the x-dependent cutoff factor $(1-x^{10})$. (This special cutoff factor is invented from the requirement that only the tails of the distribution functions are modified.) Figure 13 illustrates the effect of this tentative cutoff procedure. The solid curve here is the theoretical distribution function $\Delta u(x)-\Delta d(x)$ given as a sum of the $O(\Omega^0)$ and $O(\Omega^1)$ contributions. We point out that this distribution function is the worst case in the sense that the tail beyond $x=1$ is most significant as compared with the other distributions. The dashed curve in the same figure is obtained by using the above cutoff procedure. One sees that it leaves the distribution function for $x\leqslant 0.7$ almost intact. Naturally, this cutoff procedure alters the values of integrals of the distribution functions, i.e., the first moments. However, it turns out that the reduction is less than 2% even in the above worst case. We therefore expect that the tentative nature of the above procedure hardly affects the following qualitative analyses of scale dependence of the quark distribution functions.

For the sake of comparison, we have carried out a similar evolution procedure also for the initial distributions given by the MIT bag model. The distribution functions of the (naive) MIT bag model are already known and they are given analytically as follows [22]. The isoscalar longitudinally polarized distribution functions are given by

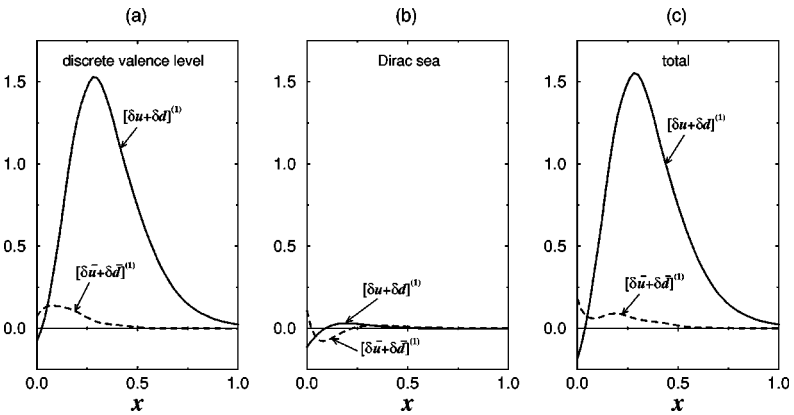

FIG. 11. The $O(\Omega^1)$ contributions to the isoscalar transversity distribution functions $\delta u(x) + \delta d(x)$ (solid curves) and $\delta\overline{u}(x) + \delta\overline{d}(x)$ (dashed curves). The meaning of the three figures (a), (b), and (c) is the same as in Fig. 2.

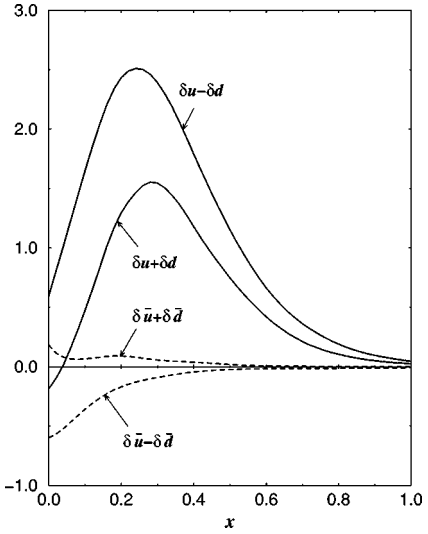

FIG. 12. The final predictions of the CQSM for the transversity distribution functions $\delta u(x)-\delta d(x)$ and $\delta\overline{u}(x)-\delta\overline{d}(x)$ given as the sums of the $O(\Omega^0)$ and $O(\Omega^1)$ contributions, in comparison with those for the isoscalar transversity distribution functions $\delta u(x)+\delta d(x)$ and $\delta\overline{u}(x)+\delta\overline{d}(x)$ coming from the $O(\Omega^1)$ terms.

$$\Delta u(x)+\Delta d(x)=\frac{(M_N R)\omega_1}{2\pi(\omega_1-1)j_0^2(\omega_1)}\times\left\{\int_{|y_{min}|}^{\infty}dyy\left[t_0^2(\omega_1,y)+2t_0(\omega_1,y)t_1(\omega_1,y)\left(\frac{y_{min}}{y}\right)+t_1^2(\omega_1,y)\left(2\left(\frac{y_{min}}{y}\right)^2-1\right)\right]\right\}, \tag{143}$$

whereas the isoscalar transversity distribution functions is given as

$$\delta u(x)+\delta d(x)=\frac{(M_N R)\omega_1}{2\pi(\omega_1-1)j_0^2(\omega_1)}\times\left\{\int_{|y_{min}|}^{\infty}dyy\left[t_0^2(\omega_1,y)+2t_0(\omega_1,y)t_1(\omega_1,y)\left(\frac{y_{min}}{y}\right)+t_1^2(\omega_1,y)\left(\frac{y_{min}}{y}\right)^2\right]\right\}. \tag{144}$$

On the other hand, the isovector distribution functions are simply related to the isoscalar ones as

$$\Delta u(x)-\Delta d(x)=\frac{5}{3}[\Delta u(x)+\Delta d(x)], \tag{145}$$

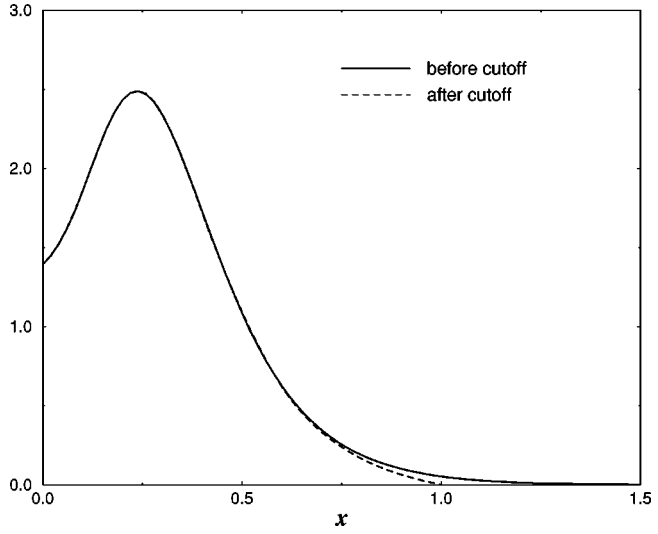

FIG. 13. The solid curve represents the theoretical distribution functions $\Delta u(x)-\Delta d(x)$, whereas the dashed curve is a modified one obtained from it by multiplying a x-dependent cutoff factor $(1-x^{10})$.

$$\delta u(x)-\delta d(x)=\frac{5}{3}[\delta u(x)+\delta d(x)]. \tag{146}$$

In Eqs. (137) and (138), M_N and R respectively stand for the nucleon mass and the bag radius, while ω_n is the nth root of the bag eigenvalue equation as

$$\tan\omega_n=-\frac{\omega_n}{\omega_n-1}, \tag{147}$$

and $y_{min}=xM_NR-\omega_1$. The function $t_l(\omega_n,y)$ is defined by

$$t_l(\omega_n,y)=\int_0^1 j_l(u\omega_n)j_l(uy)u^2du. \tag{148}$$

The bag radius R is only one free parameter of this simple model. In the numerical calculation, we adopt the value used by Jaffe and Ji [22], i.e.,

$$M_NR=4.0\omega_1, \tag{149}$$

where $\omega_1\simeq 2.043$ is the lowest (dimensionless) eigenvalue of the bag equation.

To get a rough idea about the scale dependence, we show in Fig. 14 and Fig. 15 the theoretical polarized quark distribution functions before and after Q^2 evolution. Here $\Delta u(x)$ and $\delta u(x)$ in Fig. 14(a) respectively stand for the longitudinal and transversity distributions for u-quark. In our model, the difference between the two distributions are sizable even at the initial low energy scale. A comparison with the existing and yet-to-be-obtained high energy data must be done with care, since the way of evolution of these two distributions are pretty different and the deference between the two becomes larger and larger as Q^2 increases. A general trend is a rapid growth of small x component of the longitudinally polarized distribution due to the coupling with gluons. A similar tendency is also observed for the corresponding

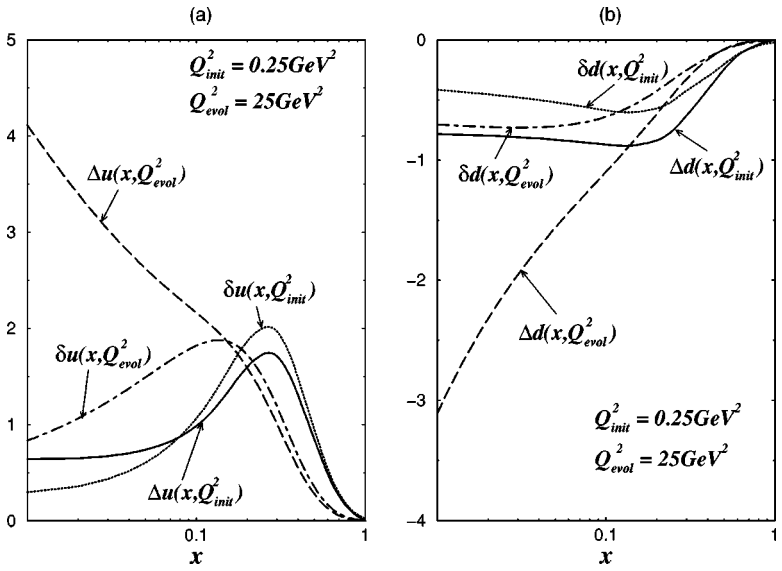

FIG. 14. The theoretical predictions for the twist-2 spin dependent quark distribution functions before and after Q^2 evolution. Here $\Delta u(x)$ and $\delta u(x)$ [in (a)] respectively stand for the longitudinal and transversity distributions of u quark, while $\Delta d(x)$ and $\delta d(x)$ [in (b)] are the corresponding quantities for d quark.

d-quark distributions shown in Fig. 14(b). We can also give some predictions for the polarized antiquark distribution functions. As one can see in Fig. 15, even the signs are different for the longitudinal and transversity distributions. (This is the case for both of $\bar{u}$ and $\bar{d}$ quarks.) The twist-2 spin dependent distribution functions were calculated by several authors based on various effective models of baryons [12,32,38–40]. As for the polarized quark distribution functions, the predictions of various models give more or less similar shape of distributions assuming that they take account of the dominant nature of the valence quark contribution as well as the effects of pion cloud in some effective way. The situation is quite different for the polarized *antiquark* distributions. The transversity distribution functions for the antiquarks have, for instance, been evaluated by Barone *et al.* within the chiral chromodielectric model [39]. Comparing their predictions for $\delta\bar{u}(x)$ and $\delta\bar{d}(x)$ with ours shown in Fig. 15, we find that their model gives $\delta\bar{u}(x)>0$, while ours does $\delta\bar{u}(x)<0$. The shapes of $\delta\bar{u}(x)$ and $\delta\bar{d}(x)$ are also quite different in both models. In consideration of the fact that the polarized antiquark distributions are quite sensitive to the detailed dynamics of the model, it is very important to get precise phenomenological information for them.

Next we show in Fig. 16(a) the theoretical predictions for the proton structure function $g_1^p(x,Q^2)$ at $Q^2=5\ \mathrm{GeV}^2$ in comparison with the corresponding experimental data given by E143 Collaboration [41]. The theoretical curves are obtained as follows. Starting with the initial distributions $\Delta u(x)+\Delta d(x)$, $\Delta\bar{u}(x)+\Delta\bar{d}(x)$ and $\Delta u(x)-\Delta d(x)$, $\Delta\bar{u}(x)-\Delta\bar{d}(x)$ or equivalently $\Delta u(x),\Delta\bar{u}(x)$ and $\Delta d(x),\Delta\bar{d}(x)$ given at $Q^2_{init}\simeq 0.25\,\mathrm{GeV}^2$ [we assume $\Delta s(x)=\Delta\bar{s}(x)=0$ and $\Delta g(x)=0$ at this energy scale], we solve the NLO evolution equation to obtain the distribution functions at $Q^2=5\ \mathrm{GeV}^2$. These distribution functions are then convoluted with the relevant quark and gluon coefficient functions at the NLO within the framework of perturbative QCD. These procedures have been carried out for the initial distribution given by the CQSM and also by the MIT bag model. The solid and dashed curves in Fig. 16(a) respectively stand for the prediction of the CQSM and that of the MIT bag model. A remarkable feature of the CQSM as compared with the MIT bag model is the enhancement of the structure function at small x region, i.e., large sea quark components. One also observes that a clear peak of $g_1^p(x,Q^2)$ around $x\simeq 0.3$ predicted by the MIT bag model (a relativistic valence quark model) is not seen in the experimental structure function. On the other hand, one can say that the prediction of the CQSM reproduces qualitative feature of the observed structure function in the whole range of x. Figure 16(b) shows the theoretical prediction of the CQSM (solid curve) and that of the MIT bag model (dashed curve) for the neutron spin structure function $g_1^n(x,Q^2)$ in comparison with the E154 data [42]. One clearly sees that the neutron spin structure function $g_1^n(x,Q^2)$ predicted by the MIT bag model is negligibly small in magnitude even after evolution. We recall that at the initial energy scale the naive MIT bag model predict $g_1^n(x)=0$, which is a necessary consequence of a model that does not properly incorporate chiral symmetry. On the other hand, the prediction of the CQSM for $g_1^n(x,Q^2)$ is seen to be large and negative especially in the small x region in good agreement with the experimental observation. Then, this agreement may be regarded as a manifestation of the importance of chiral symmetry in the physics of high-energy deep-inelastic scattering.

As is widely known, the simplest but the most important quantities characterizing the quark distribution functions are the associated first moments. Here we are interested in the first moments of the longitudinally polarized distribution functions and of the transversity ones, which are respectively called the axial and tensor charges defined as

$$g_A^{(3)}=\int_0^1\{[\Delta u(x)-\Delta d(x)]+[\Delta\bar{u}(x)-\Delta\bar{d}(x)]\}dx, \tag{150}$$

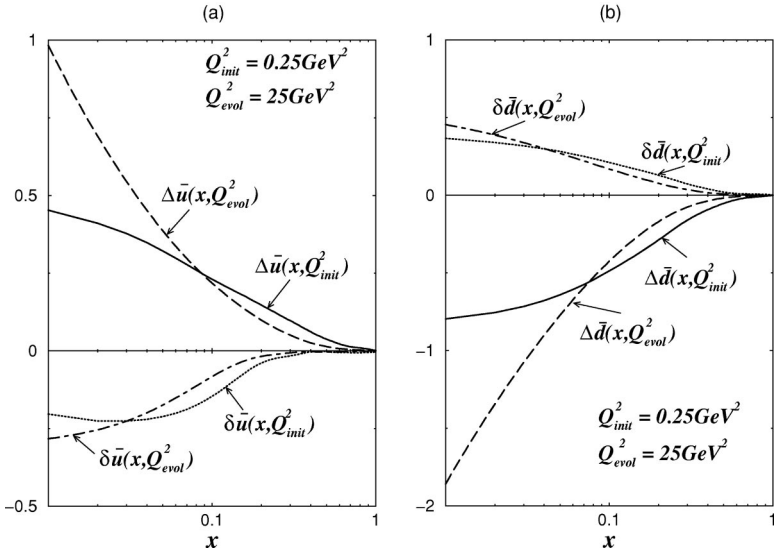

FIG. 15. The theoretical predictions for the twist-2 spin dependent antiquark distribution functions before and after Q^2 evolution. Here $\Delta\overline{u}(x)$ and $\delta\overline{u}(x)$ [in (a)] respectively stand for the longitudinal and transversity distributions of $\overline{u}$ quark, while $\Delta\overline{d}(x)$ and $\delta\overline{d}(x)$ [in (b)] are the corresponding quantities for $\overline{d}$ quark.

$$g_A^{(0)} = \int_0^1 \{[\Delta u(x) + \Delta d(x)] + [\Delta\overline{u}(x) + \Delta\overline{d}(x)]\}dx, \tag{151}$$

$$g_T^{(3)} = \int_0^1 \{[\delta u(x) - \delta d(x)] - [\delta\overline{u}(x) - \delta\overline{d}(x)]\}dx, \tag{152}$$

$$g_T^{(0)} = \int_0^1 \{[\delta u(x) + \delta d(x)] - [\delta\overline{u}(x) + \delta\overline{d}(x)]\}dx. \tag{153}$$

Before discussing the prediction of the CQSM for these quantities, it may be instructive to remember some basic properties of those. (We recall that the first calculation of the tensor charge in the CQSM was given in [43].) As emphasized by Jaffe and Ji [22], there is a remarkable difference between the axial and tensor charges originating from the charge conjugation properties of the relevant operators. For each flavor, the tensor charge counts the number of valence quarks (quarks *minus* antiquarks) of opposite transversity. Consequently, the sea quarks do not contribute to the tensor charge. (This does not necessarily means vanishing transverse polarization of antiquarks, however.) On the other hand, the axial charge counts the number of quarks *plus* antiquarks of opposite helicity. In fact, by rewriting Eqs. (152) and (153) as

$$g_A^{(3)} = \int_0^1 \{[\Delta u(x) - \Delta d(x)] - [\Delta\overline{u}(x) - \Delta\overline{d}(x)]\}dx + 2\int_0^1 [\Delta\overline{u}(x) - \Delta\overline{d}(x)]dx, \tag{154}$$

$$g_A^{(0)} = \int_0^1 \{[\Delta u(x) + \Delta d(x)] - [\Delta\overline{u}(x) + \Delta\overline{d}(x)]\}dx + 2\int_0^1 [\Delta\overline{u}(x) + \Delta\overline{d}(x)]dx, \tag{155}$$

the first and the second terms of the above equation can respectively be interpreted as valence and sea quark contri-

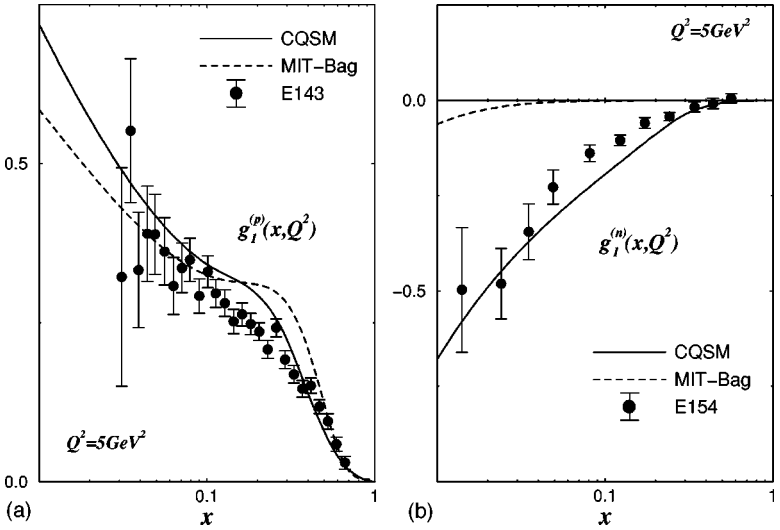

FIG. 16. The theoretical predictions for the proton and neutron spin structure functions $g_1^p(x,Q^2)$ and $g_1^n(x,Q^2)$ at $Q^2 = 4$ GeV^2 in comparison with the corresponding SLAC data. The solid and dashed curves in (a) respectively stand for the prediction of the CQSM and that of the naive MIT bag model for $g_1^p(x,Q^2)$, whereas the black circles are the E143 data [41]. The corresponding theoretical predictions for the $g_1^n(x,Q^2)$ are shown in (b) together with the E154 data [42].

TABLE I. The theoretical predictions for the isovector and isoscalar axial charges as well as the corresponding tensor charges. The predictions of the MIT bag model and those of the lattice QCD [44] are also shown together with some experimental data [45,46].

	CQSM	MIT-bag	Lattice QCD [44]	Experiment
$g_A^{(3)}$	1.41	1.06	0.99	1.254 ± 0.006 [45] (Q^2-indep.)
$g_A^{(0)}$	0.35	0.64	0.18	0.31 ± 0.07 [46] ($Q^2 = 10\ \mathrm{GeV}^2$)
$g_T^{(3)}$	1.22	1.34	1.07	–
$g_T^{(0)}$	0.56	0.80	0.56	–
$g_A^{(0)}/g_A^{(3)}$	0.25	0.60	0.18	0.24
$g_T^{(0)}/g_T^{(3)}$	0.46	0.60	0.52	–

butions in the parton model. Since the sea quark degrees of freedom is absent in the nonrelativistic framework, the difference between the axial and tensor charges is purely relativistic. Still, one must clearly distinguish two types of relativistic effect. The one is dynamical effects, which generate sea quark polarization. The other is kinematical effects, which make a difference between the axial and tensor charges even though the sea quark degrees of freedom are totally neglected. The existence of this latter effect can readily be convinced by comparing the prediction of two ''valence quark models,'' i.e., the nonrelativistic (constituent) quark model and the MIT bag model. In fact, the nonrelativistic quark model predicts

$$g_A^{(3)} = g_T^{(3)} = \frac{5}{3}, \tag{156}$$

$$g_A^{(0)} = g_T^{(0)} = 1, \tag{157}$$

while the prediction of the MIT bag model is given by

$$g_A^{(3)} = \frac{5}{3} \cdot \int \left(f^2 - \frac{1}{3} g^2 \right) r^2 dr,$$
$$g_T^{(3)} = \frac{5}{3} \cdot \int \left(f^2 + \frac{1}{3} g^2 \right) r^2 dr, \tag{158}$$

$$g_A^{(0)} = 1 \cdot \int \left(f^2 - \frac{1}{3} g^2 \right) r^2 dr,$$
$$g_T^{(0)} = 1 \cdot \int \left(f^2 + \frac{1}{3} g^2 \right) r^2 dr, \tag{159}$$

where f and g are upper and lower components of the lowest energy quark wave functions. For a typical bag radius $R \simeq 4.0 \omega_1 / M_N$, which was used before, this gives

$$g_A^{(3)} \simeq 1.06, \quad g_T^{(3)} \simeq 1.34, \tag{160}$$

$$g_A^{(0)} \simeq 0.64, \quad g_T^{(0)} \simeq 0.80. \tag{161}$$

As is obvious from Eqs. (158) and (159), the splittings of the axial and tensor charges are due to the different sign of the lower component (p-wave) contributions [22]. One should however notice that there is one interesting feature shared by both the nonrelativistic quark model and the MIT bag model. The predictions of the both models for the ratio of the isoscalar to isovector axial charges as well as the ratio of the isoscalar to isovector tensor charges are just the same:

$$g_A^{(0)}/g_A^{(3)} = g_T^{(0)}/g_T^{(3)} = 3/5. \tag{162}$$

Although there is no experimental information yet for the tensor charges, the above prediction for the ratio of the two axial charges obviously contradicts the EMC observation.

Now we shall argue that the above prediction may be interpreted as showing the limitation of simple valence quark models, which fail to properly incorporate chiral symmetry of QCD. To convince it, we compare in Table I the predictions of the NRQM and the MIT bag model with those of the CQSM, which maximally incorporate chiral symmetry. For the sake of reference, the predictions of the lattice QCD are also shown [44]. (Here we have omitted the errors of the lattice QCD calculation, for simplicity.) We first point out that the predictions of the CQSM for the above ratios, i.e.,

$$g_A^{(0)}/g_A^{(3)} \simeq 0.25, \quad g_T^{(0)}/g_T^{(3)} \simeq 0.46, \tag{163}$$

strongly deviate from the above predictions of the two valence quark models. What is remarkable here is that the CQSM predicts very small isoscalar axial charge in consistent with the EMC observation. (More meaningful comparison should be made after taking account of the scale dependence of this quantity.) Its prediction for the isovector axial charge is also qualitatively consistent with the experimental value determined from the neutron beta decay. (The deviation from the experimental value is only about 11%.) The lattice gauge theory also predicts a very small isoscalar axial charge $g_A^{(0)} \simeq 0.18$. However, this prediction may not be taken as a final one since it largely underestimates the isovector axial charge. At any rate, one can observe qualitative similarities between the predictions of the CQSM and those of the lattice QCD. Both predicts quite a small number for the ratio of the isoscalar to isovector axial charges as compared with the prediction $g_A^{(0)}/g_A^{(3)} = 0.6$ of the NRQM or the MIT bag model. On the other hand, the predictions of both models for the ratio of the isoscalar to isovector charges is not extremely different from the prediction $g_T^{(0)}/g_T^{(3)} = 0.6$ of

the latter valence quark models. In our opinion, the observed deviation from the valence quark picture indicates an importance of chiral symmetry as a generator of ''dynamical sea quark effect,'' and the predicted feature is expected to be confirmed by future measurements of tensor charges.

To compare the theoretical first moments of the spin distribution functions with the existing data for the longitudinal case and with yet-to-be-observed ones for the transversity case, we must take account of the scale dependence of the relevant moments. As is well known, the first moment of the isovector longitudinal distribution functions, i.e., the isovector axial charge is scale independent, i.e., it does not evolve: $g_A^{(3)}(Q^2)=g_A^{(3)}(Q_{init}^2)$. This is due to the conservation of the flavor nonsinglet axial-vector current [52]. This is not generally the case for the flavor singlet (isoscalar) axial charge owing to the so-called axial anomaly of QCD [47,48]. (Still, one can take a scheme called the chiral invariant factorization scheme in which the flavor singlet axial charge is independent of Q^2 [49]. Here, we take more standard gauge invariant factorization scheme [50].) In the singlet sector, the nth moments of the longitudinally polarized distribution functions are coupled with the corresponding gluon contributions. The evolution of these nth moments is governed by the anomalous dimension matrix

$$\gamma^{(p)n}\equiv\begin{pmatrix}\gamma_{qq}^{(p)n} & \gamma_{qg}^{(p)n}\\ \gamma_{gq}^{(p)n} & \gamma_{gg}^{(p)n}\end{pmatrix}, \tag{164}$$

where $\gamma^{(0)}$ and $\gamma^{(1)}$ are 1- and 2-loop contributions to the anomalous dimensions. An analytic solution to this coupled evolution equation of the NLO is given in the matrix form [51,52]:

$$\Gamma^n(Q^2)=\begin{pmatrix}\Delta\Sigma^n(Q^2)\\ \Delta G^n(Q^2)\end{pmatrix}, \tag{165}$$

$$\Gamma^n(Q^2)=\left\{\left(\frac{\alpha_s(Q^2)}{\alpha_s(Q_{init}^2)}\right)^{\Lambda_-^n/2\beta_0}\left[P_-^n-\frac{1}{2\beta_0}\frac{\alpha_s(Q_{init}^2)-\alpha_s(Q^2)}{4\pi}P_-^n\gamma^nP_-^n\right.\right.$$
$$\left.\left.-\left(\frac{\alpha_s(Q_{init}^2)}{4\pi}-\frac{\alpha_s(Q^2)}{4\pi}\left(\frac{\alpha_s(Q^2)}{\alpha_s(Q_{init}^2)}\right)^{(\lambda_+^n-\lambda_-^n)/2\beta_0}\right)\frac{P_-^n\gamma^nP_+^n}{2\beta_0+\lambda_+^n-\lambda_-^n}\right]+(+\leftrightarrow-)\right\}\Gamma^n(Q_{init}^2). \tag{166}$$

Here $\alpha_s(Q^2)$ is the QCD running coupling constant at the next-to-leading order with $\overline{\rm MS}$ scheme, β_0 and β_1 are the 1- and 2-loop QCD beta functions, respectively, and

$$\gamma^n=\gamma^{(1)n}-\frac{\beta_1}{\beta_0}\gamma^{(0)n}. \tag{167}$$

$P_\pm^n$ are 2×2 projection matrices defined by

$$P_\pm^n=\pm(\gamma^{(0)n}-\lambda_\mp^n\hat{1})/(\lambda_+^n-\lambda_-^n), \tag{168}$$

with $\hat{1}$ being a 2×2 unit matrix and with

$$\lambda_\pm^n=\frac{1}{2}[\gamma_{qq}^{(0)n}+\gamma_{gg}^{(0)n}\pm\sqrt{(\gamma_{qq}^{(0)n}-\gamma_{gg}^{(0)n})^2+4\gamma_{qg}^{(0)n}\gamma_{gq}^{(0)n}}], \tag{169}$$

the eigenvalues of the 1-loop anomalous dimension matrix $\gamma^{(0)n}$. Since the necessary anomalous dimension matrices are all given in [52], it is easy to calculate the Q^2 evolution of the first moment of the flavor singlet longitudinally polarized distribution functions, i.e., the isosinglet axial charge.

Because of its chiral-odd nature, the moments of the transversity distributions do not couple with gluons, irrespective of the flavor quantum numbers, which especially means that isovector and isoscalar tensor charges follow the same evolution equation. The anomalous dimension of the transversity distribution at the leading 1-loop order was first given by Artru and Mekhfi [53], while the corresponding 2-loop contributions have recently been given by three groups independently [54–56]. Once the relevant anomalous dimensions are known, it is easy to obtain an analytical solution of the NLO evolution equation for the nth moment of transversity distribution. Here, we use the form given by Hayashigaki *et al.* [55] as

$$\frac{\delta q_1^{(n)}(Q^2)}{\delta q_1^{(n)}(Q_{init}^2)}=\left(\frac{\alpha_s(Q^2)}{\alpha_s(Q_{init}^2)}\right)^{\gamma_h^{(0)n}/2\beta_0}\left(\frac{\beta_0+\beta_1\frac{\alpha_s(Q^2)}{4\pi}}{\beta_0+\beta_1\frac{\alpha_s(Q_{init}^2)}{4\pi}}\right)^{(1/2)(\gamma_h^{(1)n}/\beta_1-\gamma_h^{(0)n}/\beta_0)}, \tag{170}$$

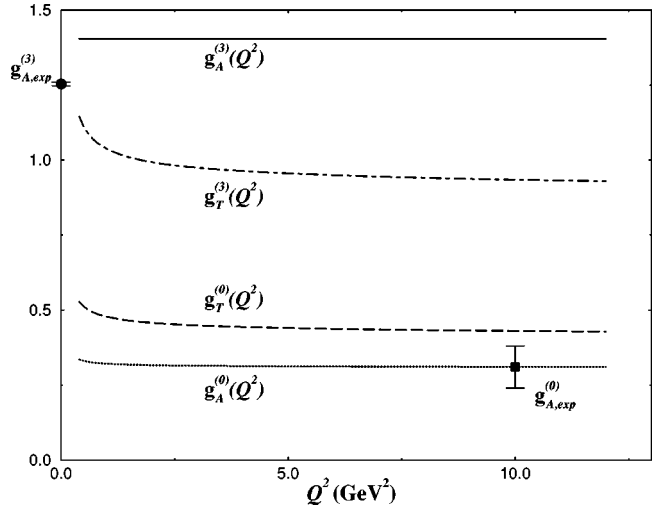

FIG. 17. The scale dependence of the axial and tensor charges. The evolution equations at the next-to-leading order are solved under the initial conditions $g_A^{(3)}(Q_{init}^2)=1.41$, $g_A^{(0)}(Q_{init}^2) \equiv \Delta\Sigma(Q_{init}^2)=0.35$, $g_T^{(3)}(Q_{init}^2)=1.22$, $g_T^{(0)}(Q_{init}^2)=0.56$, and $\Delta G(Q_{init}^2)=0$ at $Q_{init}^2=0.25\,\mathrm{GeV}^2$.

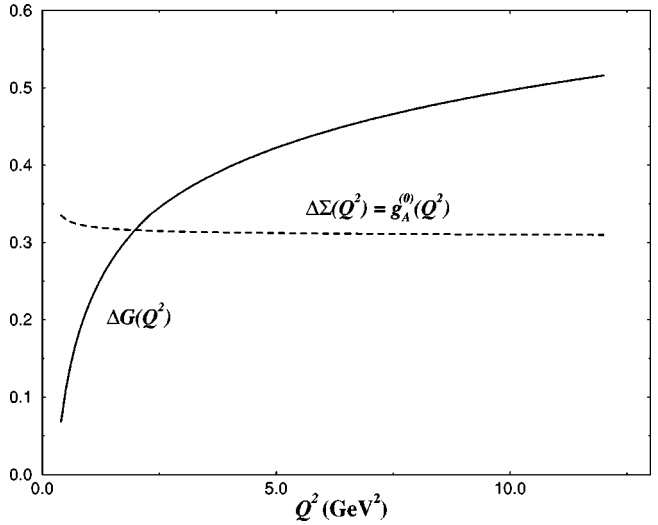

FIG. 18. The scale dependence of the flavor singlet axial charge (or the quark polarization) and the gluon polarization. The initial conditions for the evolution equation are the same as given in Fig. 17.

where the relevant anomalous dimensions $\gamma_h^{(0)n}$ and $\gamma_h^{(1)n}$ are all given in [55]. Figure 17 show the calculated Q^2 dependence of the axial and tensor charges. For obtaining it, we start with the theoretical first moments given at the initial energy scale $Q_{init}^2=0.25\,\mathrm{GeV}$:

$$g_A^{(3)}(Q_{init}^2)=1.41, \tag{171}$$

$$g_A^{(0)}(Q_{init}^2)\equiv\Delta\Sigma(Q_{init}^2)=0.35, \tag{172}$$

$$\Delta G(Q_{init}^2)=0, \tag{173}$$

$$g_T^{(3)}(Q_{init}^2)=1.22, \tag{174}$$

$$g_T^{(0)}(Q_{init}^2)=0.56. \tag{175}$$

One sees that the Q^2 dependence of the flavor singlet axial charge is very small (it is almost constant except in the very low Q^2 region). A characteristic prediction of the CQSM for the axial charges, i.e., large isovector charge and small isoscalar charge appears to be qualitatively consistent with the corresponding experimental data at the relevant energy scale. As was pointed out by many authors [39,53–56], the Q^2 dependence of the tensor charges are sizably large. Although there is no experimental information for these latter quantities, this Q^2 dependence must be taken seriously when comparing the theoretical prediction of low energy models with future experimental date. (Note, however, that the ratio $g_T^{(0)}/g_T^{(3)}$ is Q^2 independent.)

Because of the coupling between the flavor singlet axial charge (the longitudinal quark polarization) and the gluon polarization in the evolution equation, nonzero gluon polarization appears at high Q^2 even if we have assumed $\Delta G=0$ at the initial energy scale of $Q_0^2=0.25\,\mathrm{GeV}^2$. We show in Fig. 18 the Q^2 evolution of ΔG in comparison with that of $\Delta\Sigma=g_A^{(0)}$. One sees that the gluon polarization rapidly grows with increasing Q^2. Already at $Q^2\simeq 2\,\mathrm{GeV}^2$, ΔG is seen to be larger than $\Delta\Sigma$. As explained in [50], the growth of the gluon polarization with Q^2 can be traced back to the positive sign of the anomalous dimension $\gamma_{qg}^{(0)1}$ at the leading order ($\gamma_{qg}^{(0)1}=2$). The positivity of this quantity means that a polarized quark is preferred to radiate a gluon with helicity parallel to the quark polarization. Since the net quark spin component in the proton is positive, it follows that $\Delta G>0$ at least for the gluons perturbatively emitted from quarks [50]. It is hoped that the direct information on $\Delta g(x,Q^2)$ from the di-jet asymmetry analyses at HERA in conjunction with the precise NLO analyses of $g_1(x,Q^2)$ will soon provide us with an accurate determination of the polarized gluon distribution as well as its first moment [57].

V. SUMMARY

In summary, we have shown that the CQSM naturally explains qualitative behavior of the experimentally measured longitudinally polarized structure functions of the proton and the neutron. As was shown in our previous papers, the model also reproduces an excess of $\bar{d}$ sea over the $\bar{u}$ sea in the proton very naturally [17–19]. (More complete theoretical treatment of the Gottfried sum has recently been given in [20].) Furthermore, it predicts qualitative difference between the transversity distribution functions and longitudinally polarized distribution functions. For example, in simple valence quark models like the NRQM or the MIT bag model, the ratios of the isoscalar to isovector charges are just the same for both of the axial charges and the tensor charges. On the contrary, in the CQSM or in the lattice gauge theory, this ratio turns out to be much smaller for the axial charges than for the tensor charges. In our viewpoint, what makes this difference is ''dynamical sea quark effects'' dictated by the spontaneous chiral symmetry breaking of the QCD vacuum.

Another noteworthy prediction of the CQSM is the opposite (spin) polarization of the $\bar{u}$ and $\bar{d}$ sea quarks, thereby indicating SU(2) asymmetric sea quark polarization. These observations then indicate that nonperturbative QCD dynamics due to the spontaneous chiral symmetry breaking would *survive* and manifest itself in the isospin (or flavor) dependence of high energy spin observables, especially in that of the polarized (as well as unpolarized) *antiquark* distribution functions.

ACKNOWLEDGMENTS

The authors would like to express their gratitude to T. Watabe at Ruhr Universität Bochum for useful discussion on the importance of nonlocality corrections in time. Numerical calculation was performed by using the workstations at the Laboratory of Nuclear Studies, and those at the Research Center for Nuclear Physics, Osaka University.

[1] EMC Collaboration, J. Aschman *et al.*, Phys. Lett. B **206**, 364 (1988); Nucl. Phys. **B328**, 1 (1989).
[2] F. E. Close, *An Introduction to Quarks and Partons* (Academic, London, 1979); T. Muta, *Foundations of Quantum Chromodynamics* (World Scientific, Singapore, 1987).
[3] M. Gockeler, H. Oelrich, P. E. L. Rakow, G. Schierholz, R. Horsley, E. M. Ilgenfritz, H. Perlt, and A. Schiller, J. Phys. G **22**, 703 (1996); M. Gockeler, R. Horsley, L. Mankiewicz, H. Perlt, P. Rakow, G. Schierholz, and A. Schiller, Phys. Lett. B **414**, 340 (1997); C. Best, M. Gockeler, R. Horsley, L. Mankiewicz, H. Perlt, P. Rakow, A. Schafer, G. Schierholz, A. Schiller, S. Schramm, and P. Stephenson, hep-ph/9706502.
[4] D. I. Diakonov, V. Yu. Petrov, and P. V. Pobylitsa, Nucl. Phys. **B306**, 809 (1988).
[5] M. Wakamatsu and H. Yoshiki, Nucl. Phys. **A524**, 561 (1991).
[6] For reviews, see, M. Wakamatsu, Prog. Theor. Phys. Suppl. **109**, 115 (1992); Chr. V. Christov, A. Blotz, H.-C. Kim, P. Pobylitsa, T. Watabe, Th. Meissner, E. Ruiz-Arriola, and K. Goeke, Prog. Part. Nucl. Phys. **37**, 91 (1996); R. Alkofer, H. Reinhardt, and H. Weigel, Phys. Rep. **265**, 139 (1996).
[7] A. Bramon, Riazuddin, and M. D. Scadron, J. Phys. G **24**, 1 (1998).
[8] M. Wakamatsu, Phys. Lett. B **300**, 152 (1993).
[9] J. D. Sullivan, Phys. Rev. D **5**, 1732 (1972).
[10] E. M. Henley and G. A. Miller, Phys. Lett. B **251**, 453 (1990).
[11] S. Kumano, Phys. Rev. D **43**, 59 (1991); S. Kumano and J. T. Londergan, *ibid.* **44**, 717 (1991).
[12] H. Weigel, L. Gamberg, and H. Reinhardt, Mod. Phys. Lett. A **11**, 3021 (1996); Phys. Lett. B **399**, 287 (1997); L. Gamberg, H. Reinhardt, and H. Weigel, Phys. Rev. D **58**, 054014 (1998).
[13] D. I. Diakonov, V. Yu. Petrov, P. V. Pobylitsa, M. V. Polyakov, and C. Weiss, Nucl. Phys. **B480**, 341 (1996).
[14] D. I. Diakonov, V. Yu. Petrov, P. V. Pobylitsa, M. V. Polyakov, and C. Weiss, Phys. Rev. D **56**, 4069 (1997).
[15] K. Tanikawa and S. Saito, Nagoya Univ. Report No. DPNU-96-37 (1996).
[16] NMC Collaboration, P. Amaudruz *et al.*, Phys. Rev. Lett. **66**, 2712 (1991).
[17] M. Wakamatsu and T. Kubota, Phys. Rev. D **57**, 5755 (1998).
[18] M. Wakamatsu, Phys. Rev. D **44**, R2631 (1991); Phys. Lett. B **269**, 394 (1991); Phys. Rev. D **46**, 3762 (1992).
[19] M. Wakamatsu, in *Weak and Electromagnetic Interactions in Nuclei (WEIN-92)*, Proceeding of the International Seminar, Dubna, Russia, 1992, edited by Ts. D. Vylov (World Scientific, Singapore, 1993).
[20] P. V. Pobylitsa, M. V. Polyakov, K. Goeke, T. Watabe, and C. Weiss, Phys. Rev. D **59**, 034024 (1999).
[21] J. C. Collins and D. E. Soper, Nucl. Phys. **B194**, 445 (1982); J. Kogut and D. Soper, Phys. Rev. D **1**, 2901 (1970).
[22] R. L. Jaffe and X. Ji, Nucl. Phys. **B375**, 527 (1992).
[23] R. L. Jaffe, lectures given at Ettore Majorana International School of Nucleon Structure, 1995, hep-ph/9602236.
[24] M. Wakamatsu, Prog. Theor. Phys. **95**, 143 (1996).
[25] D. I. Diakonov and V. Yu. Petrov, Nucl. Phys. **B272**, 457 (1986).
[26] C. Weiss and K. Goeke, hep-ph/9712447.
[27] S. Kahana and G. Ripka, Nucl. Phys. **A429**, 462 (1984); S. Kahana, G. Ripka, and V. Soni, *ibid.* **A415**, 351 (1984).
[28] F. Döring, A. Blotz, C. Schüren, T. Meissner, E. Ruiz-Arriola, and K. Goeke, Nucl. Phys. **A415**, 351 (1984).
[29] M. Wakamatsu and T. Watabe, Phys. Lett. B **312**, 184 (1993).
[30] Chr. V. Christov, A. Blotz, K. Goeke, P. Pobylitsa, V. Yu. Petrov, M. Wakamatsu, and T. Watabe, Phys. Lett. B **325**, 467 (1994).
[31] M. Glück, E. Reya, M. Stratmann, and W. Vogelsang, Phys. Rev. D **53**, 4775 (1996).
[32] P. V. Pobylitsa and M. V. Polyakov, Phys. Lett. B **389**, 350 (1996).
[33] M. Miyama and S. Kumano, Comput. Phys. Commun. **94**, 185 (1996).
[34] M. Hirai, S. Kumano, and M. Miyama, Comput. Phys. Commun. **108**, 38 (1998).
[35] M. Hirai, S. Kumano, and M. Miyama, Comput. Phys. Commun. **111**, 150 (1998).
[36] R. L. Jaffe, Phys. Lett. **93B**, 313 (1980); Ann. Phys. (N.Y.) **132**, 32 (1981).
[37] L. Gamberg, H. Reinhardt, and H. Weigel, Int. J. Mod. Phys. A **13**, 5519 (1998).
[38] B. L. Ioffe and A. Khodjamiriann, Phys. Rev. D **51**, 3373 (1995).
[39] V. Barone, T. Calarco, and A. Drago, Phys. Lett. B **390**, 287 (1997).
[40] K. Suzuki and T. Shigetani, Nucl. Phys. **A626**, 886 (1997); K. Suzuki and W. Weise, *ibid.* **A634**, 141 (1998).
[41] E143 Collaboration, K. Abe *et al.*, Phys. Rev. D **58**, 112003 (1998).
[42] E154 Collaboration, K. Abe *et al.*, Phys. Rev. Lett. **79**, 26 (1997).
[43] H.-C. Kim, M. Polyakov, and K. Goeke, Phys. Lett. B **387**, 577 (1996).

[44] Y. Kuramashi, Nucl. Phys. **A629**, 235c (1998); see also, M. Fukugita, Y. Kuramashi, M. Okawa, and A. Ukawa, Phys. Rev. Lett. **75**, 2092 (1995); S.-J. Dong, J.-F. Lagaë, and K.-F. Liu, *ibid.* **75**, 2096 (1995); S. Aoki, M. Doui, T. Hatsuda, and Y. Kuramashi, Phys. Rev. D **56**, 433 (1997).
[45] Particle Data Group, C. Caso *et al.*, Eur. Phys. J. C **3**, 1 (1998).
[46] J. Ellis and M. Karliner, Phys. Lett. B **341**, 397 (1995).
[47] G. Altarelli and G. G. Ross, Phys. Lett. B **212**, 391 (1988).
[48] R. D. Carlitz, J. C. Collins, and A. H. Mueller, Phys. Lett. B **214**, 229 (1988).
[49] G. T. Bodwin and J. Qiu, Phys. Rev. D **41**, 2755 (1990).
[50] For review, see H.-Y. Cheng, Int. J. Mod. Phys. A **11**, 5109 (1996).
[51] W. Furmanski and R. Petronzio, Z. Phys. C **11**, 293 (1982).
[52] M. Glück, E. Reya, and A. Vogt, Z. Phys. C **48**, 471 (1990).
[53] X. Artru and M. Mekhfi, Z. Phys. C **45**, 669 (1990).
[54] S. Kumano and M. Miyama, Phys. Rev. D **56**, 2504 (1997).
[55] A. Hayashigaki, Y. Kanazawa, and Y. Koike, Phys. Rev. D **56**, 7350 (1997).
[56] W. Vogelsang, Phys. Rev. D **57**, 1886 (1998).
[57] A. De Roeck, A. Deshpande, V. W. Huges, J. Lichtenstadt, and G. Rädel, Eur. Phys. J. C **6**, 121 (1999).